


## Determining the Optimal Percentage of FRP Composite Bars in Hybrid Reinforced Beams

Kaveh Karami<sup>1</sup>; Jalil Shafaei<sup>1</sup>; Mojtaba Lezgy-Nazargah<sup>2,\*</sup> 

1. Faculty of Civil Engineering, Shahrood University of Technology, Shahrood 3619995161-316, Iran

2. Department of Civil Engineering, Faculty of Engineering, Hakim Sabzevari University, Sabzevar 9617976487-397, Iran

\* Corresponding author: [m.lezgy@hsu.ac.ir](mailto:m.lezgy@hsu.ac.ir)

### ARTICLE INFO

#### Article history:

Received: 23 January 2025

Revised: 10 March 2025

Accepted: 11 June 2025

#### Keywords:

HSF-reinforced concrete beams;

FRP composite bar;

Steel bar;

Residual deformation;

Ductility.

### ABSTRACT

Reinforcing the concrete beams with the combination of steel and FRP composite bars improves the structural performance and long-term durability of these members significantly. Although hybrid steel-FRP (HSF) reinforced concrete (RC) beams have better structural behaviors than those members reinforced only with pure steel or pure FRP composite bars, no comprehensive research has been reported on determining the optimal percentage of steel and FRP composite bars in RC beams yet. Filling this gap is the main aim of the present study. To reach this aim, the sectional analysis of a series of HSF-reinforced concrete beams under different loading stages has been carried out, and the moment-curvature relationships in considered beams have been determined. Different values have been considered for the percentage of tensile steel, FRP composite, and compressive steel bars. Various values are also considered for the compressive strength of concrete, the yield stress of steel bars, and the mechanical properties of the FRP composite bars. To find suitable structural performance, the moment-curvature curves of concrete beams reinforced with HSF bars were compared with each other. Reducing residual deformations as well as increasing ductility are chosen as a criterion for determining the optimal percentage of steel and composite bars and other design parameters of the HSF-reinforced concrete beams. Results of this research show that the use of the optimum percentage of steel and FRP bars improves the flexural capacity, the desired ductility, and the corrosion resistance of the RC beams, and meanwhile, reduces the effects of residual deformations.

E-ISSN: 2345-4423

© 2025 The Authors. Journal of Rehabilitation in Civil Engineering published by Semnan University Press.

This is an open access article under the CC-BY 4.0 license. (<https://creativecommons.org/licenses/by/4.0/>)

#### How to cite this article:

Karami, K., Shafaei, J. and Lezgy Nazargah, M. (2026). Determining the Optimal Percentage of FRP Composite Bars in Hybrid Reinforced Beams. Journal of Rehabilitation in Civil Engineering, 14(2), 2249  
<http://doi.org/10.22075/jrce.2025.2249>

## 1. Introduction

To compensate the weak resistance of concrete against tensile forces, it is necessary to reinforce concrete structures with appropriate materials. Steel bars are widely used in RC structures due to their abundance, ductility, and proportionality of their elasticity modulus with concrete. However, the corrosion of steel bars is one of their weak aspects for use in RC structures [1]. On the other hand, composite bars made of fiber-reinforced polymer (FRP) display good corrosion resistance. They have good mechanical characteristics such as low weight, high tensile strength, and non-magnetic properties. For the reasons mentioned above, in the last two decades, FRP composite bars have been widely used instead of steel bars for reinforcing concrete. However, the main disadvantage of FRP composite bars is their brittleness. FRP materials display the linear response before they reach the ultimate strength. The brittle behavior of FRP bars is a limitation that prevents ductile and non-linear responses of concrete structures reinforced with these materials [2,3], [4].

Depending on the amounts of FRP composite bars, the failure modes of FRP-reinforced concrete structures are different. The low reinforcement ratios of FRP lead to the failure of bars before the concrete crushing. When the amount of FRP used for reinforcing concrete is high, the concrete is crushed under compression, while the tensile stresses in FRP bars remain less than their ultimate resistance. For this reason, most design codes recommend using the high percentage values of FRP for reinforcing the concrete members to ensure the occurrence of plastic deformations in compressive concrete and increase ductility. Moreover, to have an alarm before the collapsing of such members, the possibility of plastic deformations in the compressive concrete is essential. In other words, in FRP-reinforced concrete structures, it is better the failure of FRP composite bars to take place after the concrete crushing [5]. In addition to the lack of ductility, FRP bars have a lower elastic modulus than steel bars. Due to this reason, FRP-reinforced concrete structures have more significant deflection and greater crack width under service loads in comparison to steel-reinforced concrete structures. For the design of concrete structures reinforced with FRP bars, it is necessary to control the behavior of such structures in the serviceability limit state in addition to their control in the ultimate limit state [6], [7], [8].

The combination of steel and FRP bars for reinforcing the concrete structures is a practical solution to overcome the low ductility and serviceability drawbacks of FRP-reinforced concrete structures [9], [10], [11]. The use of HSF systems for reinforcing concrete structures has extensively increased in the last decade. In a hybrid reinforcing system, steel bars increase the ductility of the concrete structure and decrease their creep. On the other hand, FRP bars improve the flexural and corrosion resistance of the host concrete structures and reduce their residual deformations. The use of steel/FRP bars for reinforcing concrete structures is a relatively new research field. HSF-reinforced beams integrate the advantages of both steel and FRP materials to improve the performance of structural elements. These hybrid beams are widely employed in real-world applications where high durability, lighter weight, and resistance to environmental degradation are essential. HSF-reinforced beams are particularly beneficial in bridge construction, especially in environments exposed to de-icing salts or marine conditions. The FRP components greatly minimize the risk of corrosion compared to traditional steel reinforcement. In marine structures such as piers, jetties, and docks, where exposure to seawater causes severe corrosion, HSF-reinforced beams offer an optimal solution. The FRP reinforcement remains unaffected by the corrosive effects of saltwater and moisture, while the steel provides the necessary structural strength. HSF-reinforced beams are also well-suited for overpasses and tunnels in areas with heavy traffic or harsh environmental conditions. In industrial or coastal regions where buildings face exposure to aggressive chemicals, moisture, or salts, HSF-reinforced beams deliver exceptional resistance to degradation while maintaining structural integrity. Additionally, HSF-reinforced beams are highly advantageous in parking garages located in coastal or cold climates, where salt and moisture are common causes of corrosion. In

summary, HSF-reinforced concrete beams are particularly valuable in environments where durability, corrosion resistance, and weight reduction are critical. Their use in bridges, marine structures, industrial settings, and other applications enhances the performance and longevity of infrastructure while lowering maintenance and operational costs. Recent studies related to the structural behavior of HSF-reinforced concrete beams have been briefly reviewed in the following paragraphs.

Aiello and Ombres [11] experimentally investigated the flexural behavior of concrete beams reinforced with a combination of AFRP and steel bars. In this reference, steel and AFRP bars with the same cross-sectional area are placed in the tensile region of the concrete beams in different layers. Aiello and Ambres found that adding steel bars to an AFRP-reinforced cross-section significantly increases the ductility of the beam and reduces the width and spacing of cracks. Leung and Balendran [12] conducted an experimental study on the load-deflection behavior of concrete beams reinforced with GFRP and steel bars. They tested seven rectangular beams with a length of 5.2 meters with two different arrangements of steel and GFRP bars. The experimental results of these researchers showed that the yielding of steel bars occurs in all specimens. They also found that the flexural capacity of the concrete beam reinforced with hybrid bars increases by increasing the GFRP reinforcement ratio. Qu *et al.* [13] studied experimentally and numerically the flexural behavior of hybrid GFRP-steel RC beams. They tested eight beams, including two reference beams reinforced with pure steel and pure GFRP bars, and six concrete beams reinforced with hybrid steel-GFRP bars. The amount of reinforcements and the ratio of GFRP to steel bars were two main parameters which are investigated by Qu and his colleagues. They found that using steel reinforcement in combination with GFRP bars improves the structural performance of concrete beams so that the flexural stiffness of the beams increases while the beams display enough ductility. Sun *et al.* [14] investigated the flexural behavior of concrete beams reinforced with different bars. The considered reinforcements include standard steel bars, pure FRP bars (BFRP and CFRP), and HSF composite bars. The results of these researchers showed that HSF-reinforced concrete beams display proper and stable hardening behavior after the yielding of steel bars, and concrete crushing in them occurs after the rupture of the outermost FRP bar. The results of Ref. [14] also showed that the steel-reinforced concrete beam has the highest ductility coefficient. However, its ultimate load-bearing capacity is approximately 31 percent of the flexural capacity of HSF-reinforced concrete beams. El Refai *et al.* [15] investigated the structural performance of HSF-reinforced concrete beams. They studied the flexural behavior of six concrete beams reinforced with a combination of steel and GFRP bars, as well as three beams reinforced with pure GFRP bars. These researchers found that using steel bars in combination with GFRP bars generally improves the flexural behavior of the concrete beams. Ductility, cracking pattern, hardness, and load capacity are among the parameters that are improved.

In order to ensure the use of steel and FRP in sufficient amounts in concrete sections and to ensure the sufficient resistance and ductility of RC members, Pang *et al.* [16] proposed formulas and equations for the design of concrete beams reinforced with steel and GFRP bars. Pang and colleagues found that the compressive strength of concrete, the strength of steel, the type of FRP, the effective stiffness of reinforcements, and the ultimate compressive strain of concrete are among the most critical parameters that significantly affect the ductility of the RC beam. By using the finite element method, Qin *et al.* [17] studied the effect of the hybrid reinforcement ratio on the flexural performance of concrete beams. They considered both over- and under-reinforced beams and validated their numerical models through comparison with the experimental results of Lau and Pam [18]. In Qin *et al.* [17], the hybrid reinforcement ratio ( $A_f/A_s$ ) in the range between 1 and 2.5 is recommended for ensuring the sufficient ductility and suitable flexural capacity of concrete beams in non-linear regimes. It is also recommended in Ref. [17] that the needed amount of reinforcements should be designed firstly according to ACI440.1R-15 with the assumption that only FRP bars exist in the beam. Then, the required amount of replacing steel

bars should be calculated according to the suggested range  $1 < A_f/A_s < 2.5$ . Mustafa and Hassan [19] investigated the bending behavior of HSF-reinforced concrete beams using nonlinear finite element modeling. They showed that the simultaneous existence of steel and FRP bars in concrete members leads to improvement of ductility, elimination of undesirable failure modes, and better performance during initiation and propagation of cracks. Sun *et al.* [20] experimentally investigated the flexural behavior of five concrete beams reinforced with different types and arrangements of steel and BFRP bars. The results of this research showed that after the yielding of steel bars, the flexural capacity of the beam increases uniformly. Moreover, due to the presence of FRP bars, a significant and stable secondary stiffness appears in the concrete beam. Sun *et al.* [20] also found that the secondary stiffness in beams whose bars are arranged close together is higher than those beams whose bars are placed in a spaced and far apart manner.

Kim and Kim [21] studied the structural behavior of six HSF-reinforced concrete beams using experimental tests. The reinforcing bars (steel-steel, steel-GFRP, and steel-CFRP) and the grade of concrete (40 MPa, and 60 MPa) of these six beams were different from each other. Results of Ref. [21] show that the flexural strength of HSF-reinforced specimens is about two times of pure steel-reinforced specimens. They also found that the maximum deflections corresponding to the ultimate flexural strength of HSF-reinforced specimens are increased by 86 up to 116 percent in comparison to pure steel-reinforced specimens. Ge *et al.* [22] experimentally investigated the flexural performance of eight HSF-reinforced concrete beams. They found that the flexural strength and stiffness of this type of beam increases compared to beams that are reinforced only with FRP bars. Using equilibrium equations and the principle of compatibility of strains, Ge and colleagues presented an analytical formulation for predicting the flexural behavior of HSF-reinforced concrete beams. Moolaei *et al.* [4] experimentally studied the behavior of concrete beams reinforced with steel and GFRP bars. They substituted the conventional concrete with high-performance fiber-reinforced cementitious composites (HPFRCC). Three groups of beams (beams with only GFRP bars, beams with only steel bars, and beams with hybrid steel/GFRP bars) were subjected to the four-point bending test. They found that HPFRCC concrete significantly increases the flexural capacity, ductility, and energy absorption of HSF-reinforced concrete beams. Structural responses of seven hybrid steel/BFRP-reinforced concrete beams under the four-point bending loading test were studied by Liu *et al.* [23]. The percentage of reinforcement in six concrete beam samples was lower than the balanced section, while the reinforcement ratio in one reinforced concrete beam specimen was slightly greater than the balanced value. The results of Liu *et al.* [23] show that hybrid concrete beams whose reinforcement ratios are below the balanced value have more considerable deflections and larger crack widths. The ductility index of under-reinforced beams is also relatively greater than hybrid steel/FRP over-reinforced concrete beams.

In summary, the review of open literature shows that the main drawbacks of the concrete beams reinforced with FRP bars are high deflections under service loads, large crack width, and low ductility. To overcome the above drawbacks and improve the structural performance of RC beams, the use of FRP bars in combination with steel bars is recommended. Thanks to the structural participation of steel bars in addition to FRP bars, the ductility index and flexural stiffness of the concrete beams increase significantly. Moreover, the crack width and risk of collapse due to corrosion are effectively reduced. To achieve the desired structural aims mentioned above, the accurate and optimal determination of FRP/steel reinforcement ratios in concrete beams is necessary. Despite the importance of this issue, no comprehensive and complete study has been reported in the past research. Determining the appropriate type of FRP bars (e.g., GFRP, CFRP, and AFRP) for reinforced concrete beams is another issue that has

not been discussed in the literature. Finding practical answers to the above questions is the primary goal of the present study.

In this research, an attempt has been made to determine the optimal percentage of steel/FRP bars required for reinforcing concrete beams so that the load-displacement response of the concrete beams becomes bi-linear. In pure steel-reinforced concrete members, no significant increase in flexural capacity is observed after the yielding of steel bars. The use of FRP bars in conjunction with steel bars improves the flexural stiffness of the concrete beams after the yielding phase of steel and leads to the appearance of bi-linear stiffness in such beams. Moreover, HSF-reinforced beams with bi-linear stiffness have more ductility than pure FRP-reinforced concrete beams. In determining the optimum percentage of the FRP and steel bars in the HSF-reinforced concrete beams, in addition to the appearance of bi-linear stiffness in the beam, the criterion of minimum residual deformations is also considered. Due to the elastic behavior of FRP bars, the residual deformations induced in the HSF-reinforced concrete beams are lower than in pure steel-reinforced concrete beams. Note that the rehabilitation of RC beams after severe earthquakes becomes easier by decreasing residual deformations.

To reach the objectives of the research, 10800 HSF-reinforced concrete beams with various mechanical properties and different reinforcing details are considered. The percentage of steel/FRP bars, the strength of steel/FRP bars, and the compressive strength of concrete in these beams are different from each other. The moment-curvature relationships in the considered HSF beams have been determined by using sectional analysis. By comparing the moment-curvature curves of HSF-reinforced concrete beams with each other, an attempt has been made to determine the optimal percentage of steel and FRP composite bars. Having a high ductility index and having low residual deformations are two criteria that are considered in the comparison of the moment-curvature curves.

## 2. Sectional analysis of HSF-reinforced concrete beams

In this section, the sectional analysis of HSF-reinforced concrete beams has been described. It is assumed that the concrete and steel/FRP reinforcing bars are perfectly connected so that no slip occurs at the interfaces between them. It is also assumed that the planes perpendicular to the longitudinal axis of the beam remain perpendicular after bending. In other words, the sectional analysis presented in this study is based on the assumption of the Euler-Bernoulli beam theory.

### 2.1. Constitutive equations

In this study, Hognestad's model [24] is used to represent the stress-strain relationships of concrete under compression. According to Hognestad's formulation, one can write:

$$\sigma_c = f'_c \left( \frac{2\varepsilon_c}{\varepsilon_{co}} - \left( \frac{\varepsilon_c}{\varepsilon_{co}} \right)^2 \right) \quad (1)$$

where  $\sigma_c$  is the compressive stress and  $\varepsilon_c$  is the compressive strain of the concrete.  $f'_c$  denotes the ultimate compressive strength of the cylindrical specimen, and  $\varepsilon_{co}$  is the strain corresponding to the ultimate compressive strength of concrete. Concerning the stress-strain relationships of the concrete under tension, the following linear elastic behavior is considered:

$$\sigma_t = \begin{cases} E_c \varepsilon_t & \varepsilon_t < \frac{f_t}{E_c} \\ 0 & \varepsilon_t > \frac{f_t}{E_c} \end{cases} \quad (2)$$

where  $\sigma_t$  is the tensile stress and  $\varepsilon_c$  is the tensile strain of the concrete material.  $f_t$  is the tensile strength of the concrete, and  $E_c$  denotes the modulus of elasticity of the concrete.

The following linear elastic stress-strain relationships have been considered for the behavior of FRP composite bars:

$$f_{frp} = \begin{cases} E_{frp} \varepsilon_{frp} & \varepsilon_{frp} < \varepsilon_{frp,u} \\ 0 & \varepsilon_{frp} > \varepsilon_{frp,u} \end{cases} \quad (3)$$

In the above equation,  $f_{frp}$  and  $\varepsilon_{frp}$  are the stress and strain in FRP composite bars, respectively.  $E_{frp}$  denotes the modulus of elasticity of FRP and  $\varepsilon_{frp,u}$  is the ultimate strain of FRP.

The behavior of steel bars is assumed to be ideal elastic-plastic as below:

$$f_s = \begin{cases} E_s \varepsilon_s & \varepsilon_s < \varepsilon_y \\ f_y & \varepsilon_s > \varepsilon_y \end{cases} \quad (4)$$

where  $f_s$  and  $\varepsilon_s$  are stress and strain in the steel bars, respectively.  $f_y$  is the yield stress, and  $E_s$  denotes the modulus of elasticity of steel bars.

## 2.2. Equilibrium equations

The cross-section of an HSF-reinforced concrete beam is shown in Fig. 1. In this figure, the distributions of strain and stress along the height of the beam are also shown. The equilibrium of forces along the horizontal direction gives:

$$T_{frp} + T_s + C_t = C_c + C_s \quad (5)$$

where  $T_s$  and  $T_{frp}$  denote the resultant tensile force in steel bars and FRP composite bars, respectively.  $C_c$ ,  $C_t$ , and  $C_s$  are the resultant forces in the compressive concrete, tensile concrete, and compression steel bars, respectively.

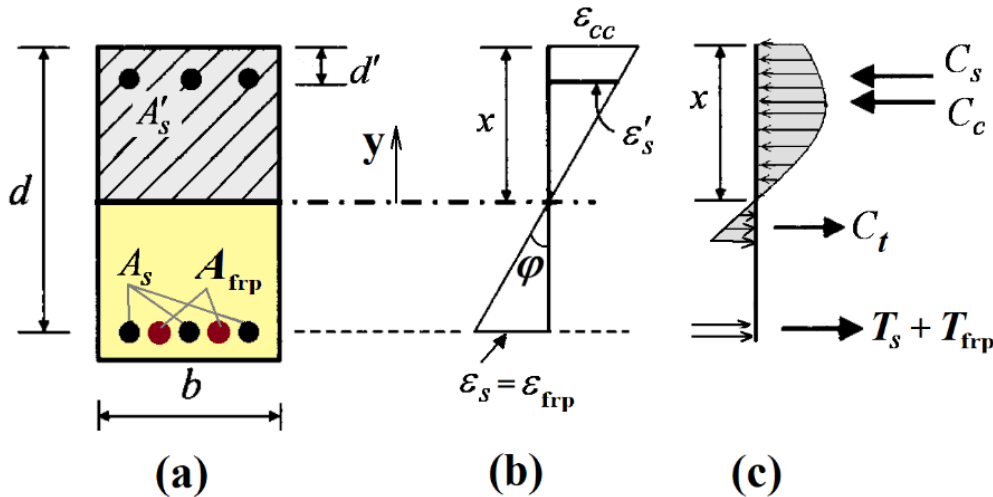


**Fig. 1.** (a) Cross-section of the HSF-reinforced concrete beam, (b) distribution of strain (c), distribution of stress.

By considering Fig. 1, Eq. (5) can be rewritten as follows:

$$A_s f_s + A_{frp} f_{frp} + \int_0^{h-x} \sigma_t b dy = \int_0^x \sigma_c b dy + A'_s f'_s \quad (6)$$

In the above equation,  $A_s$ ,  $A_{frp}$ , and  $A'_s$  are the cross-sectional area of the tensile steel bars, FRP composite bars, and compression steel bars, respectively.  $b$  is the width of the cross-section, and  $x$  is the

depth of the neutral axis. By writing the equilibrium of the moment around the tensile reinforcements, the following expression is obtained for the moment strength of the HSF-reinforced concrete beam:

$$M_r = \int_0^x \sigma_c y b dy - \int_0^{h-x} \sigma_t y b dy + A'_s f'_s (x - d') \quad (7)$$

where  $h$  represents the depth of the beam's section.

### 2.3. Compatibility of deformations

According to the strain diagram shown in Fig. 1.b, the value of the strain in tensile steel and FRP composite bars can be calculated in terms of  $x$  as below:

$$\varepsilon_s = \varepsilon_{frp} = \frac{d-x}{x} \varepsilon_{cc} \quad (8)$$

In the above relationship,  $\varepsilon_{cc}$  represents the maximum strain of the compressive concrete. Depending on the value of the load applied to the hybrid concrete beam,  $\varepsilon_{cc}$  will be a value in the range of 0 to 0.003. The strain in compression steel bars can also be calculated from the following relation:

$$\varepsilon'_s = \frac{x-d'}{x} \varepsilon_{cc} \quad (9)$$

where  $d'$  represents the distance of the extreme fiber in compression to the centroid of the compression steel bars.

### 2.4. Moment-curvature relations

After substituting constitutive equations (1)-(3) and compatibility relations (7)-(8) in Eq. (6), one can calculate the unknown depth of the neutral axis (i.e.,  $x$ ). After calculating  $x$ , the resistance moment of the section can be calculated from Eq. (7). It should be noted that in this study, the Newton-Raphson iteration method has been used for computing  $x$ . Having the value of  $x$ , the curvature of the concrete beam ( $\varphi$ ) can be calculated from the following equation:

$$\varphi = \frac{\varepsilon_{cc}}{x} \quad (10)$$

In this study, the determination of the optimal percentage of steel and FRP bars has been accomplished by evaluating the values of the maximum curvature ( $\varphi_u$ ) and residual curvature ( $\varphi_R$ ) of the analyzed concrete beams. Whatever the maximum value of curvature in a beam is greater, that beam has a higher ductility index and higher energy absorption. Also, if the residual curvature in a beam is smaller, less permanent deformations will be observed in the structure after reloading. For this purpose, the following two dimensionless indices are defined:

$$\mu = \frac{\varphi_u}{\varphi_y} \quad (11)$$

$$R = \frac{\varphi_u}{\varphi_R} \quad (12)$$

where  $\mu$  and  $R$  are ductility and residual index, respectively. In addition,  $\varphi_y$  represents the curvature corresponding to the yield moment of the HSF-reinforced concrete beam. For more clarity, the parameters  $\varphi_y$ ,  $\varphi_u$ , and  $\varphi_R$  are shown in Fig. 2. Note that the residual index defined in Eq. (12) is a new parameter introduced for the first time in this paper. Considering this new index in the design process of HSF-reinforced beams significantly reduces the retrofitting costs of these structures after the occurrence of severe earthquakes.

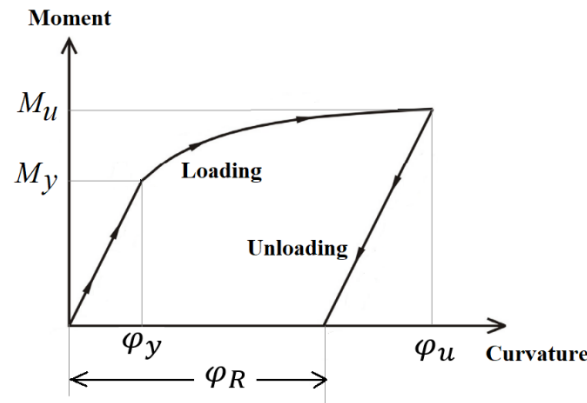


Fig. 2. Moment-curvature curve and meaning of residual curvature.

The flowchart shown in Fig. 3 visually summarizes the process of cross-sectional analysis in HSF-reinforced concrete beams.

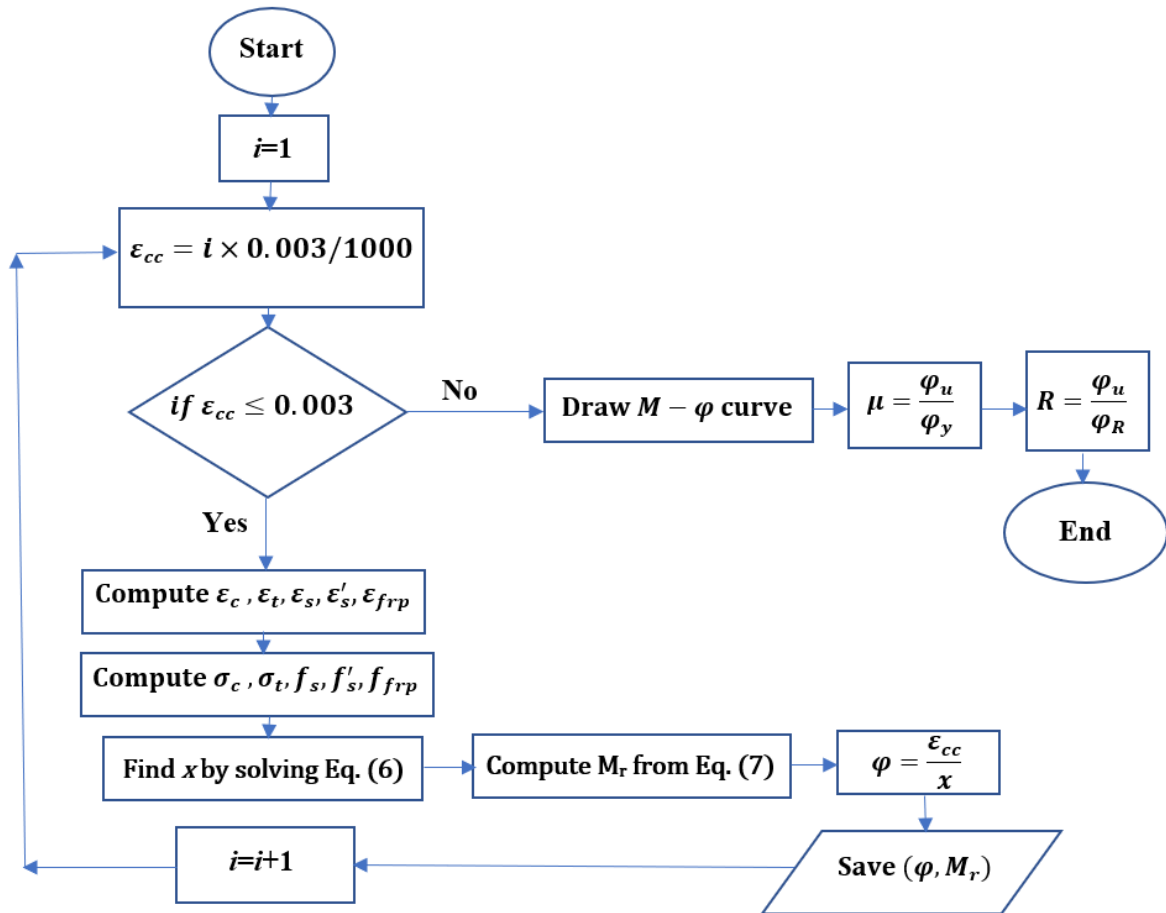


Fig. 3. Flowchart of the cross-sectional analysis process.

## 2.5. Failure modes

Research has shown that HSF-reinforced beams experience three primary flexural failure modes, depending on the ratios of FRP and steel reinforcement [25]:

- Failure Mode I: The FRP reinforcement ruptures after the tensile steel reinforcement yields, with no concrete crushing (common in lightly reinforced beams).



- Failure Mode II: Concrete crushing occurs after the tensile steel reinforcement yields, while the FRP reinforcement remains intact (typical of moderately reinforced beams).
- Failure Mode III: Concrete crushing happens while both the tensile steel and FRP reinforcement are still in the elastic state (characteristic of heavily reinforced beams).

The failure mode I is frequently observed in bridge girders and deck slabs. Failure Mode II is the most desirable among the three modes because it is more gradual and offers greater ductility or deformability compared to the other modes. In practical design, employing a "ductile beam" approach is not only cost-effective but also allows for the complete utilization of the strength properties of materials such as FRP, steel, and concrete.

The rupture strain of FRP bars is significantly higher than the yield strain of steel bars. However, due to the compatibility of deformations across the cross-section, the strains in the FRP and steel bars must be equal. Therefore, it can be concluded that the rupture of FRP bars cannot occur before the yielding of steel bars. In other words, a failure mode characterized by the conditions  $\varepsilon_{frp} = \varepsilon_{frp,u}$ ,  $\varepsilon_s \leq \varepsilon_y$ , and  $\varepsilon'_c \leq 0.003$  or  $\varepsilon'_c > 0.003$  is not possible.

## 2.6. Minimum and balanced reinforcement ratio

According to ACI 440.11-22 [26], the balanced reinforcement ratio ( $\rho_f^{bal}$ ) for the pure FRP-reinforced concrete beam is given by:

$$\rho_f^{bal} = 0.85\beta_1 \left( \frac{f'_c}{f_{u,frp}} \right) \left( \frac{\varepsilon'_c E_{frp}}{f_{u,frp} + \varepsilon'_c E_{frp}} \right) \quad (13)$$

where  $\beta_1$  denotes the ratio of the equivalent rectangular concrete stress block depth to neutral axis depth,  $\varepsilon'_c = 0.003$  is the ultimate concrete strain in compression, and  $f_{u,frp}$  denotes the ultimate strength of FRP bars. Based on ACI 318-19(22) [27], the balanced reinforcement ratio for the pure steel-reinforced concrete beam is defined as:

$$\rho_s^{bal} = 0.85\beta_1 \left( \frac{f'_c}{f_y} \right) \left( \frac{600}{600 + f_y} \right) \quad (14)$$

The minimum reinforcement ratio for the pure steel-reinforced concrete beam is given by [27]:

$$\rho_s^{min} = \min \left\{ \frac{1.4}{f_y}, \frac{3\sqrt{f'_c}}{f_y} \right\} \quad (15)$$

Current design provisions lack a clear definition for the balanced reinforcement ratio in HSF-reinforced concrete beams. Given that failure mode I is uncommon and not recommended for design purposes, the balanced reinforcement ratio for an HSF-reinforced concrete beam can be defined as a criterion to distinguish failure modes II and III from each other. In other words, a balanced condition corresponds to a specific steel content where, at the moment that the concrete crushing occurs ( $\varepsilon'_c = 0.003$ ), tensile steel reinforcement simultaneously reaches its yield strength ( $\varepsilon_s = \varepsilon_y$ ), while the FRP reinforcement remains intact without rupturing ( $\varepsilon_{frp} < \varepsilon_{frp,u}$ ). According to the equilibrium and compatibility conditions on cross-section, the balanced steel reinforcement ratio for the HSF-reinforced concrete beam can be defined as:

$$\rho_{HSF}^{bal} = 0.85\beta_1 \left( \frac{f'_c}{f_y} \right) \left( \frac{600}{600 + f_y} \right) - \frac{E_{frp}}{E_s} \rho_f \quad (16)$$

When an HSF-reinforced beam is under-reinforced, concrete crushing takes place after the tensile steel reinforcement has yielded, and the FRP reinforcement remains intact (Mode II). Conversely, when the

HSF-reinforced beam is over-reinforced, concrete crushing occurs while both the tensile steel and FRP reinforcement are still in the elastic state (Mode III).

### 3. Validation study

Based on the analytical formulations developed in section 2, a computer program has been developed in MATLAB software to calculate the relationship between bending moment and curvature in concrete beams reinforced with HSF bars. In this section, the developed computer program has been validated through comparison with similar results available in the open literature.

#### 3.1. Steel-reinforced concrete beam

In this subsection, a concrete beam reinforced with steel tensile bars has been analyzed based on the formulations described in Section 2. The mechanical characteristics of steel and concrete, as well as the geometrical characteristics of the examined concrete beam, are shown in Fig. 4.a. The beam's moment-curvature diagrams for three different reinforcement ratios 0.0052, 0.010, and 0.016, are shown in Fig. 4.b. In this figure, the results obtained from the present analytical formulation are compared with the results of Moehle [28].

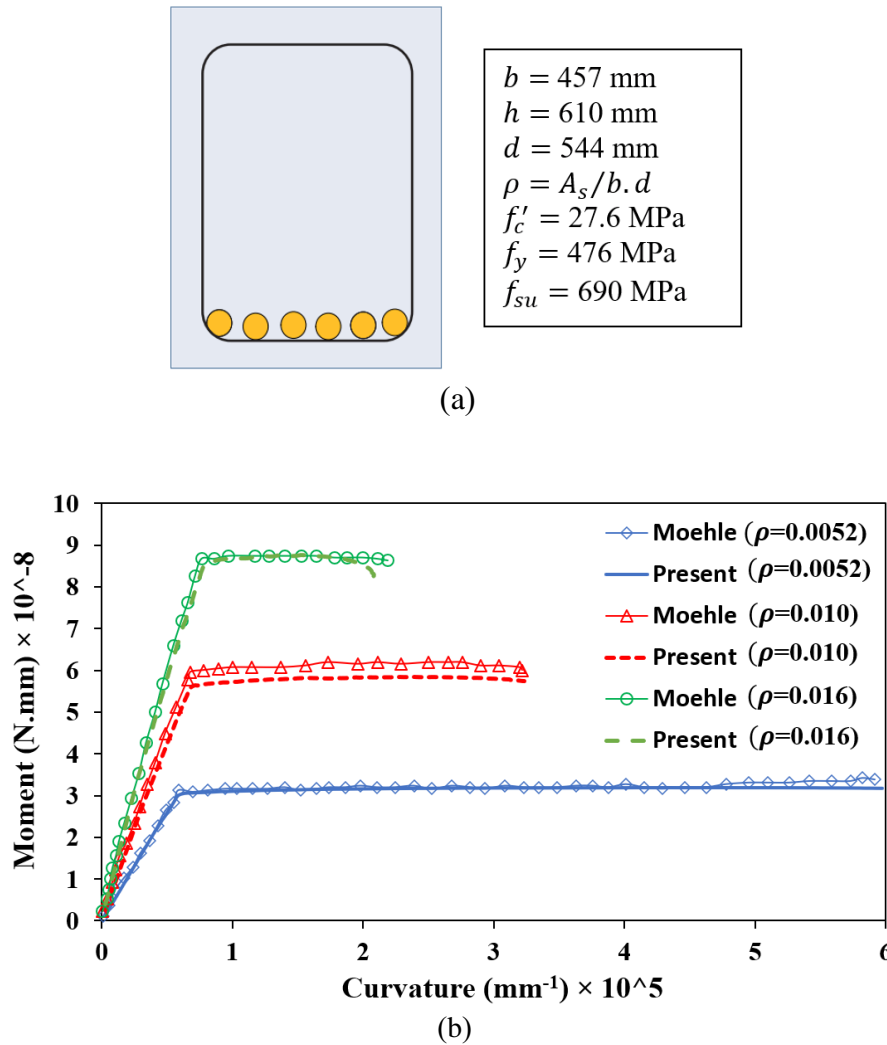


**Fig. 4.** Steel-reinforced concrete beam: (a) mechanical and geometrical characteristics, (b) moment-curvature relationships.

As seen in Fig. 4, the results of the present study are close to the results of Moehle. The maximum difference between the present results and the results of Moehle [28] is about 4%. Due to the simplifying assumptions made in the sectional analysis of HSF-reinforced concrete beams, some degree of error is anticipated in the results derived from the current model. These assumptions include a perfect bond between the steel/FRP reinforcement and concrete, an ideal bilinear elastic-plastic behavior for steel reinforcement, limiting the compressive strain of concrete to 0.003, and assuming a linear strain distribution across the cross-section. While these simplifications facilitate the analysis, they may not fully align with real-world conditions, potentially leading to discrepancies in the outcomes.

### 3.2. Doubly-steel-reinforced concrete beam

The mechanical and geometrical characteristics of the examined doubly-steel-reinforced concrete beam are shown in Fig. 5.a. The percentage of tensile reinforcements is 0.021 while three different percentages 0, 0.005, and 0.010, are assumed for the compression reinforcements. The changes in the resistance moment of the beam against its curvature are shown in Fig. 5.b. To verify the results, the present results have been compared again with the results of Moehle [28].

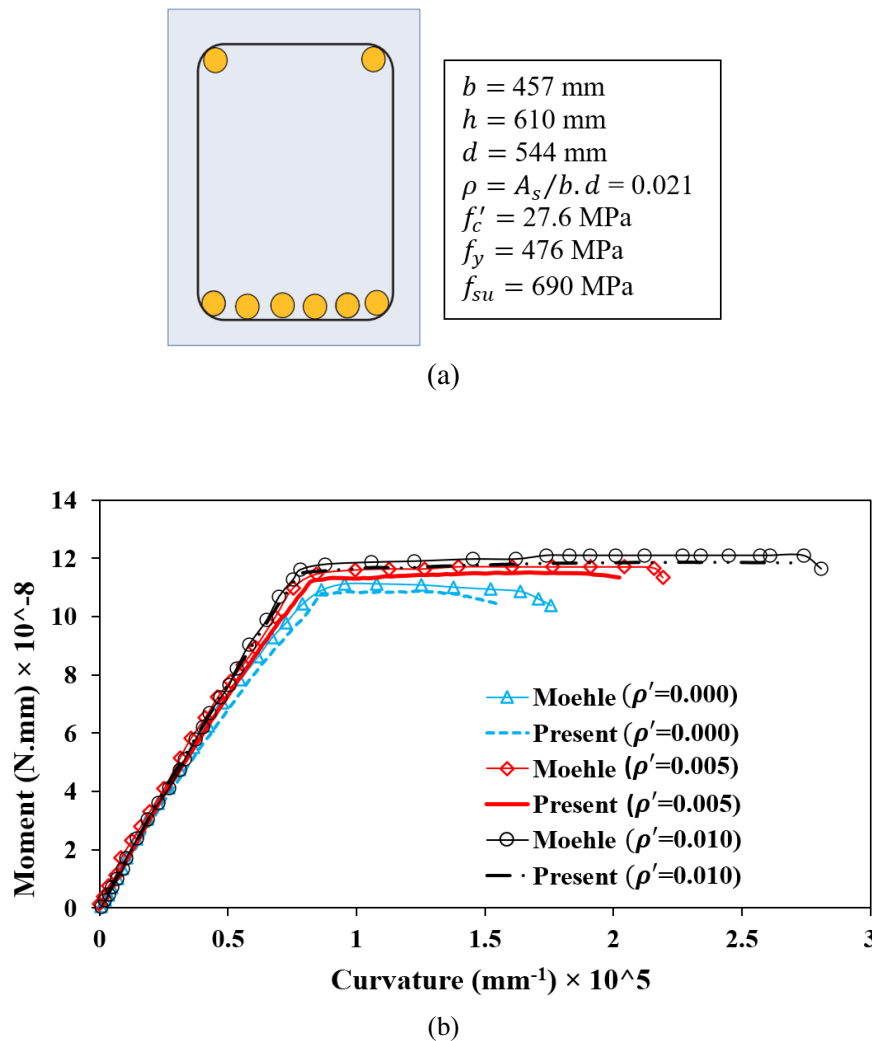


**Fig. 5.** Doubly-steel-reinforced concrete beam: (a) mechanical and geometrical characteristics, (b) moment-curvature relationships.

As can be seen in Fig. 5, the results of the present analysis are in good agreement with Moehle's results. The difference between the two sets of results in the prediction of flexural strength is less than 2%.

### 3.3. HSF-reinforced concrete beam

As the last example, a concrete beam reinforced with steel and FRP composite bars has been analyzed using the developed MATLAB code. The width of the beam is 200 mm, and its depth is 300 mm. The cross-sectional area of the steel bars is  $A_s=402 \text{ mm}^2$ , the compressive strength of concrete is  $f'_c = 35 \text{ MPa}$ , and the yield stress of steel bars is  $f_y = 480 \text{ MPa}$ . Polymeric bars are made of GFRP ( $E_{\text{frp}} = 40 \text{ GPa}$ ,  $f_u = 600 \text{ MPa}$ ) and CFRP ( $E_{\text{frp}} = 120 \text{ GPa}$ ,  $f_u = 1300 \text{ MPa}$ ). Two different values, 1 and 1.27, are assumed for the ratio of the cross-sectional area of composite bars to the cross-sectional area of steel bars. The moment-curvature relationships for steel-FRP/GFRP-reinforced concrete beams are shown in Fig. 6. In this figure, the present results are compared with the experimental results of Kara *et al.* [29].

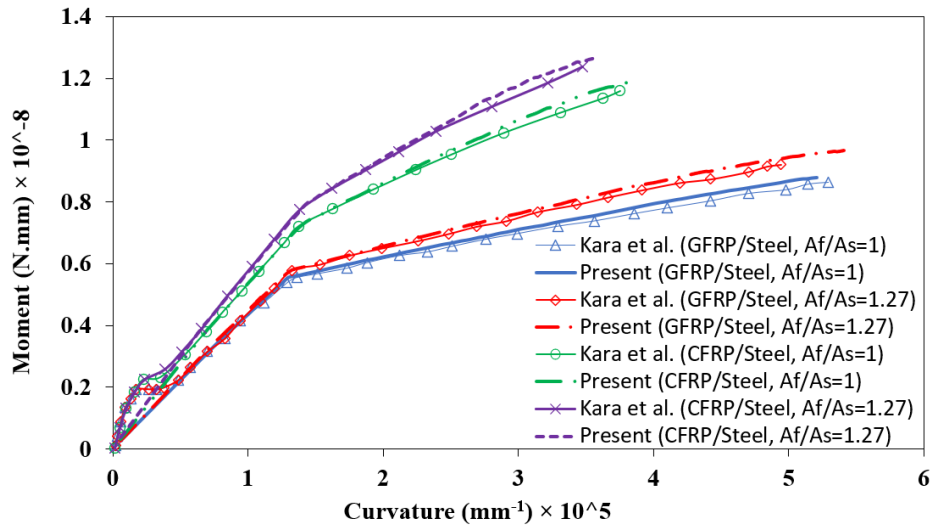


Fig. 6. Moment-curvature relationships in the hybrid steel-FRP/GFRP-reinforced concrete beams.

According to Fig. 6, it can be seen that the results obtained from the present formulation are in good agreement with experimental data. The error of the present model in predicting the flexural strength and the maximum curvature of the hybrid RC beams is 5.01% and 9.4%, respectively.

According to the above-obtained results, it can be concluded that the proposed analytical formulation, and consequently the associated MATLAB code, has sufficient accuracy for predicting moment-curvature relationships of HSF-reinforced concrete beams.

## 4. Database of modeled HSF-reinforced concrete beams

In this study, a set of 10800 HSF-reinforced concrete beams is considered. The considered HSF-reinforced concrete beams have separately been analyzed, and their moment-curvature relationships are determined. The mechanical properties and reinforcing details of the considered set of HSF-reinforced concrete beams are different from each other. The main parameters assumed for mechanical properties and reinforcing details include:

- Compressive strength of concrete
- Yield stress of steel bars
- Type of FRP composite bars
- Percentage of compression bars
- Percentage of steel bars
- Percentage of FRP composite bars

The considered values for the above-mentioned six parameters are shown in Table 1. It is seen that five distinct values for  $f'_c$ , three different values for  $f_y$ , three types of FRP, six values for  $\rho'_s$ , five values for  $\rho_s$ , and eight values for  $\rho_f$  are considered. Thus, the total number of analyzed HSF-reinforced concrete beams is equal to  $5 \times 3 \times 3 \times 6 \times 5 \times 8 = 10800$ .

**Table 1.** Considered values for main parameters of the HSF-reinforced concrete beams.

$f'_c$ (MPa)	$f_y$ (Mpa)	Type of FRP	$\rho'_s$	$\rho_s$	$\rho_f$
20	340	GFRP	0	$\rho_s^{min}$	$0.25 \times \rho_f^{bal}$
25	400	AFRP	$\rho_s^{min}$	$0.25 \times \rho_s^{bal}$	$0.5 \times \rho_f^{bal}$
30	500	CFRP	$0.25 \times \rho_s^{bal}$	$0.5 \times \rho_s^{bal}$	$0.75 \times \rho_f^{bal}$
35			$0.5 \times \rho_s^{bal}$	$0.75 \times \rho_s^{bal}$	$\rho_f^{bal}$
40			$0.75 \times \rho_s^{bal}$	$\rho_s^{bal}$	$1.25 \times \rho_f^{bal}$
			$\rho_s^{bal}$		$1.5 \times \rho_f^{bal}$
					$1.75 \times \rho_f^{bal}$
					$2 \times \rho_f^{bal}$

The geometric characteristics of the analyzed HSF beams, as well as the considered values for the cover of longitudinal reinforcements, are also shown in Table 2.

**Table 2.** Geometric characteristics and the cover of longitudinal reinforcements.

$d'$ (mm)	$d$ (mm)	$h$ (mm)	$b$ (mm)
50	450	500	400

According to Eqs. (11) and (12), whatever the dimensionless indices  $\mu$  and  $R$  are greater in a beam, the structural performance of the HSF-reinforced concrete beam against seismic loads is more suitable. In the following section, the values of dimensionless indices  $\mu$  and  $R$  are calculated for all considered HSF-reinforced concrete beams by using their moment-curvature diagrams. Then, the effects of the main parameters of HSF-reinforced concrete beams on their ductility and residual indices were investigated. Finally, based on the values obtained for the ductility and residual indices, and by using engineering judgment, the optimal values of each parameter have been determined in a way that the HSF-reinforced concrete beam has the best structural performance.

## 5. Results and discussion

In this section, the effects of various parameters (compressive strength of concrete, strength of steel bars, the mechanical properties of FRP composite bars, and the percentage of steel/FRP bars) on the energy absorption and residual deformations of HSF-reinforced concrete beams have firstly been investigated. Then, based on the results obtained from the parametric studies, the optimal percentage of the steel and FRP bars has been determined.

### 5.1. Effect of FRP reinforcement ratio on ductility and residual indices

In Fig. 7, the effect of the percentage of FRP bars on the ductility and residual indices of HSF-reinforced concrete beams has been investigated. In extracting the results of this subsection, it is assumed that  $f'_c = 35 \text{ MPa}$ ,  $f_y = 400 \text{ MPa}$ ,  $\rho_s = \rho_s^{min}$ , and composite bars are made of GFRP. Two values  $\rho'_s = 0$  and  $\rho'_s = \rho_s^{min}$  are also assumed for the percentage of steel compression bars. It has been proved later in subsections 5.2 to 5.5 that the aforementioned values considered for  $f'_c$ ,  $f_y$ ,  $\rho'_s$ ,  $\rho_s$ , and FRP's type are the most appropriate choices, which lead to the highest ductility and the lowest residual deformation in HSF-reinforced concrete beams.

As can be seen in Fig. 7, the residual index  $R$  increases with increasing the percentage of FRP composite bars while the ductility index  $\mu$  decreases. By increasing the percentage of FRP bars, the HSF-reinforced beam moves from a moderately reinforced state to a heavily reinforced one. As a result, the failure mode shifts from ductile failure mode II to brittle failure mode III, leading to a decrease in the ductility index. In beams solely reinforced with FRP bars, a similar trend takes place. As the percentage of FRP bars increases, the beam becomes over-reinforced, causing a reduction in its ductility. On the other hand, for the determination of the optimal percentage of FRP composite bar in HSF-reinforced concrete beams, it is required that both ductility and residual indices be maximum as much as possible. So, according to the reverse trend of two indices  $\mu$  and  $R$ , the FRP reinforcement ratios  $0.75 \times \rho_f^{bal}$ ,  $1 \times \rho_f^{bal}$ , and  $1.25 \times \rho_f^{bal}$ , in which both ductility and residual indices have their average value, may be considered as the optimal percentage of FRP bars.

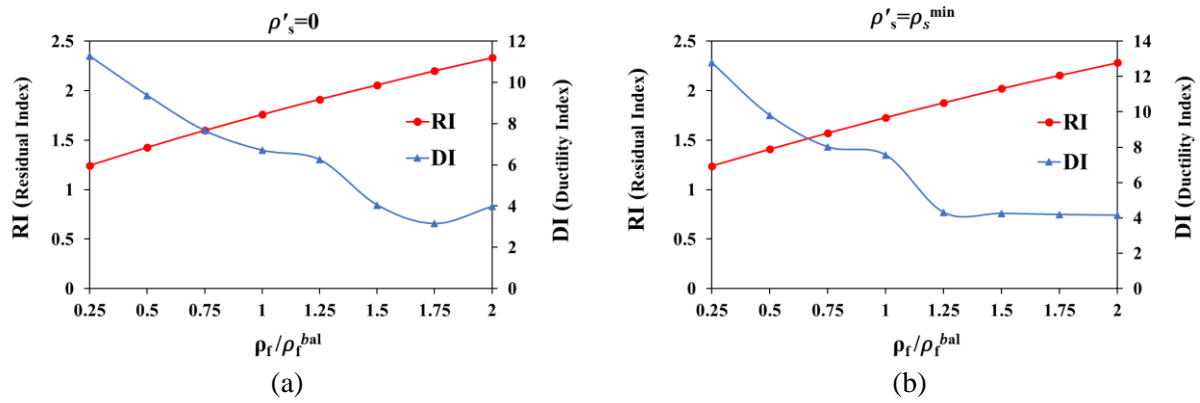


**Fig. 7.** Effect of FRP reinforcement ratio on the ductility and residual indices ( $f'_c = 35 \text{ MPa}$ ,  $f_y = 400 \text{ MPa}$ ,  $\rho_s = \rho_s^{min}$ ).

## 5.2. Effect of steel reinforcement ratio on ductility and residual indices

Fig. 8 shows the effect of the percentage of tensile steel bars on ductility and residual indices of HSF-reinforced concrete beams. It is assumed that  $f'_c = 35 \text{ MPa}$ ,  $f_y = 400 \text{ MPa}$ , and composite bars are made of the GFRP. Three values of  $0.75 \times \rho_f^{bal}$ ,  $1 \times \rho_f^{bal}$ , and  $1.25 \times \rho_f^{bal}$  are considered for FRP reinforcement ratio, and two values of  $\rho'_s = 0$  and  $\rho'_s = \rho_s^{min}$  were assumed for the reinforcement ratio of steel compression bars.

Regardless of the value of the FRP reinforcement ratio, it can be seen from Fig. 8 that the residual index of the HSF-reinforced concrete beams first decreases slightly with increasing the percentage of steel tensile bars, then increases with a gentle slope. By increasing the percentage of steel tensile bars from  $0.1 \times \rho_s^{bal}$  to  $0.25 \times \rho_s^{bal}$ , the value of the residual index decreased by about 17%. However, the value of the residual index increases by about 20% when the percentage of steel tensile bars increases from  $0.25 \times \rho_s^{bal}$  to  $1 \times \rho_s^{bal}$ . The residual index of the HSF-reinforced concrete beams is almost maximum when the value of the steel reinforcement ratio is  $0.1 \times \rho_s^{bal}$  or  $1 \times \rho_s^{bal}$ . Therefore, to minimize the permanent deformations in HSF-reinforced concrete beams, first  $1 \times \rho_s^{bal}$  and then  $0.1 \times \rho_s^{bal}$  are suitable choices for the steel reinforcement ratio. If the ductility index is considered, it can be observed from Fig. 8 that the ductility index of all HSF-reinforced concrete beams, except the beams with  $\rho'_s = \rho_s^{min}$  and  $1.25 \times \rho_f^{bal}$ , decreases with a steep slope when the percentage of tensile bars increases. By increasing the percentage of steel tensile bars from  $0.1 \times \rho_s^{bal}$  to  $1 \times \rho_s^{bal}$ , the ductility index of these beams decreases by about 300%. It seems that by increasing the percentage of steel tensile bars, the HSF section tends to become over-

reinforced, resulting in a transition in the failure mode of the HSF-reinforced beam from ductile failure mode II to brittle failure mode III. In beams solely reinforced with steel bars, a similar trend takes place. By increasing the percentage of steel tensile bars, the ductility of the beam reduces and it exhibits a brittle failure mode. It can also be seen from Fig. 8 that the ductility index of beams with  $\rho'_s = \rho_s^{min}$  and  $\rho_f = 1.25 \times \rho_f^{bal}$ , at first, increases slightly when the percentage of tensile bars reaches  $0.5 \times \rho_s^{bal}$ , then it decreases sharply. If the criterion of the maximum ductility index for all concrete beams with different  $\rho'_s$  and  $\rho_f$  is considered, it can be concluded from Fig. 8 that  $\rho_s = 0.1 \times \rho_s^{bal}$  is the most suitable choice. In other words, if the maximum ductility criterion is alone considered for determining the optimal percentage of tension bar in the HSF-reinforced concrete beams, the answer will be  $\rho_s = 0.1 \times \rho_s^{bal}$ . Since both ductility and residual indices should be as maximum as possible, according to the previous discussion about the variations of the residual index, the value  $\rho_s = 0.1 \times \rho_s^{bal}$  is finally recommended as the optimal value of the steel reinforcement ratio.

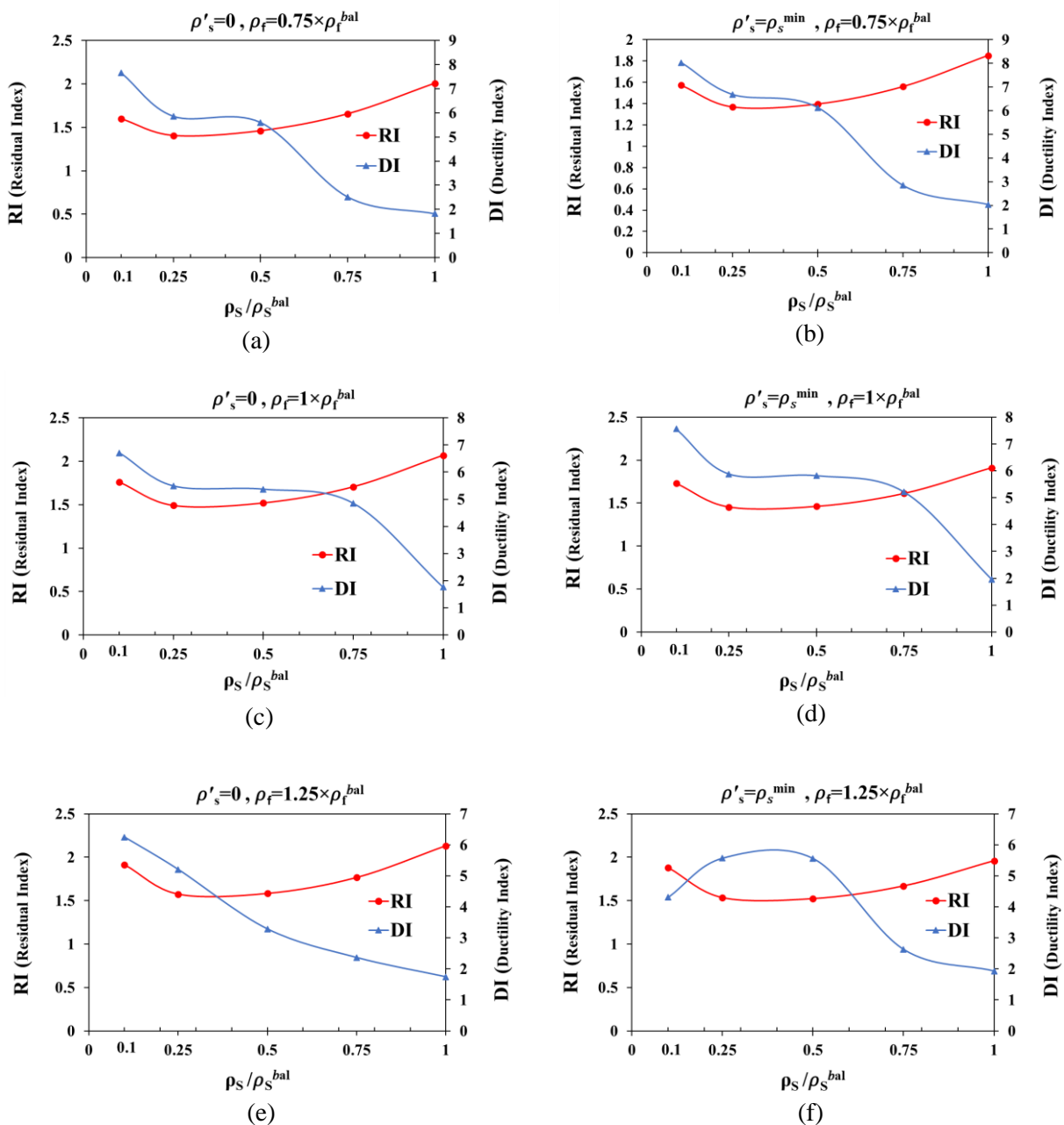


**Fig. 8.** Effect of steel reinforcement ratio on the ductility and residual indices ( $f'_c = 35 \text{ MPa}$ ,  $f_y = 400 \text{ MPa}$ ).

### 5.3. Effect of concrete strength on ductility and residual indices

In Fig. 9, the effect of the compressive strength of concrete on ductility and residual indices of HSF-reinforced concrete beams has been investigated. In extracting the results of this subsection, it is assumed that  $f_y = 400 \text{ MPa}$ ,  $\rho_s = \rho_s^{\min}$ , and composite bars are made of GFRP. Three values of  $0.75 \times \rho_f^{\text{bal}}$ ,  $1 \times \rho_f^{\text{bal}}$ , and  $1.25 \times \rho_f^{\text{bal}}$  were considered for the FRP reinforcement ratio, and two values of  $\rho'_s = 0$  and  $\rho'_s = \rho_s^{\min}$  are assumed for the reinforcement ratio of steel compression bars.

As seen in Fig. 9, the residual index of all beams increases with increasing the compressive strength of the concrete. Under a constant bending moment, the depth of the neutral axis in the HSF-reinforced concrete beams reduces by increasing the compressive strength of the concrete. Indeed, by increasing the compressive strength of concrete, the internal compressive force of concrete (i.e.,  $C_c$ ) may be increased without any significant increase in the depth of the compressive zone. According to Eq. (9), the maximum curvature of the concrete beam (i.e.,  $\varphi_u$ ) increases with the reduction of the depth of the compressive zone, leading to an increase in the residual index. So, if the criterion of minimum residual deformations is alone considered, the value of  $f'_c = 40$  is the best choice for the compressive strength of concrete.

In the following, the effect of concrete strength on the ductility index of the HSF-reinforced concrete beams has been investigated. It can be observed from Fig. 9 that the ductility index of the beams with  $\rho'_s = 0$  and  $\rho_f = 0.75 \times \rho_f^{\text{bal}}$  increases with the increase of the strength of concrete, so in these beams,  $f'_c = 40 \text{ MPa}$  is the most suitable choice if only energy absorption criterion is considered. The ductility index of the beams with  $\rho'_s = \rho_s^{\min}$  and  $\rho_f = 0.75 \times \rho_f^{\text{bal}}$  is maximum when  $f'_c < 35 \text{ MPa}$ . According to the graphs depicted in Fig. 9, it is also seen that the ductility index of the beams with  $\rho'_s = 0$  and  $\rho_f = 1 \times \rho_f^{\text{bal}}$  is maximum when the compressive strength of concrete is within the ranges of  $30 \text{ MPa} < f'_c < 35 \text{ MPa}$ . For beams with  $\rho'_s = \rho_s^{\min}$  and  $\rho_f = 1.25 \times \rho_f^{\text{bal}}$ , this range is  $25 \text{ MPa} < f'_c < 35 \text{ MPa}$ . For the beams with  $\rho'_s = 0$  and  $\rho_f = 1.25 \times \rho_f^{\text{bal}}$ , and also the beams with  $\rho'_s = \rho_s^{\min}$  and  $\rho_f = 1 \times \rho_f^{\text{bal}}$ , the value of the ductility index is maximum when the concrete strength is within the range of  $35 \text{ MPa} < f'_c < 40 \text{ MPa}$ .

If the overlap of the intervals mentioned above is considered, it can be deduced that the ductility index of all HSF-reinforced concrete beams is almost maximum when the value of the compressive strength is  $f'_c = 35 \text{ MPa}$ . Therefore, by considering the criterion of maximum ductility index alone, it can be deduced that  $f'_c = 35 \text{ MPa}$  is the most suitable choice for the compressive strength of concrete.

It is well-known that high-strength concrete typically requires higher-quality materials, including higher-grade cement, supplementary cementitious materials (like silica fume or fly ash), and high-range water-reducing admixtures (superplasticizers). These materials can increase the cost of the concrete mix. The need for precise mix designs and quality control can add to the cost. High-strength concrete also requires more skilled labor and specialized equipment for placement and curing. The aforementioned limitations often restrict the use of high-strength concrete in practical applications. If cost consideration, along with criteria of maximum ductility and minimum residual deformations are taken into account simultaneously, it can be concluded that the value of  $f'_c = 35$  is the best choice for the concrete's strength of HSF-reinforced concrete beams.



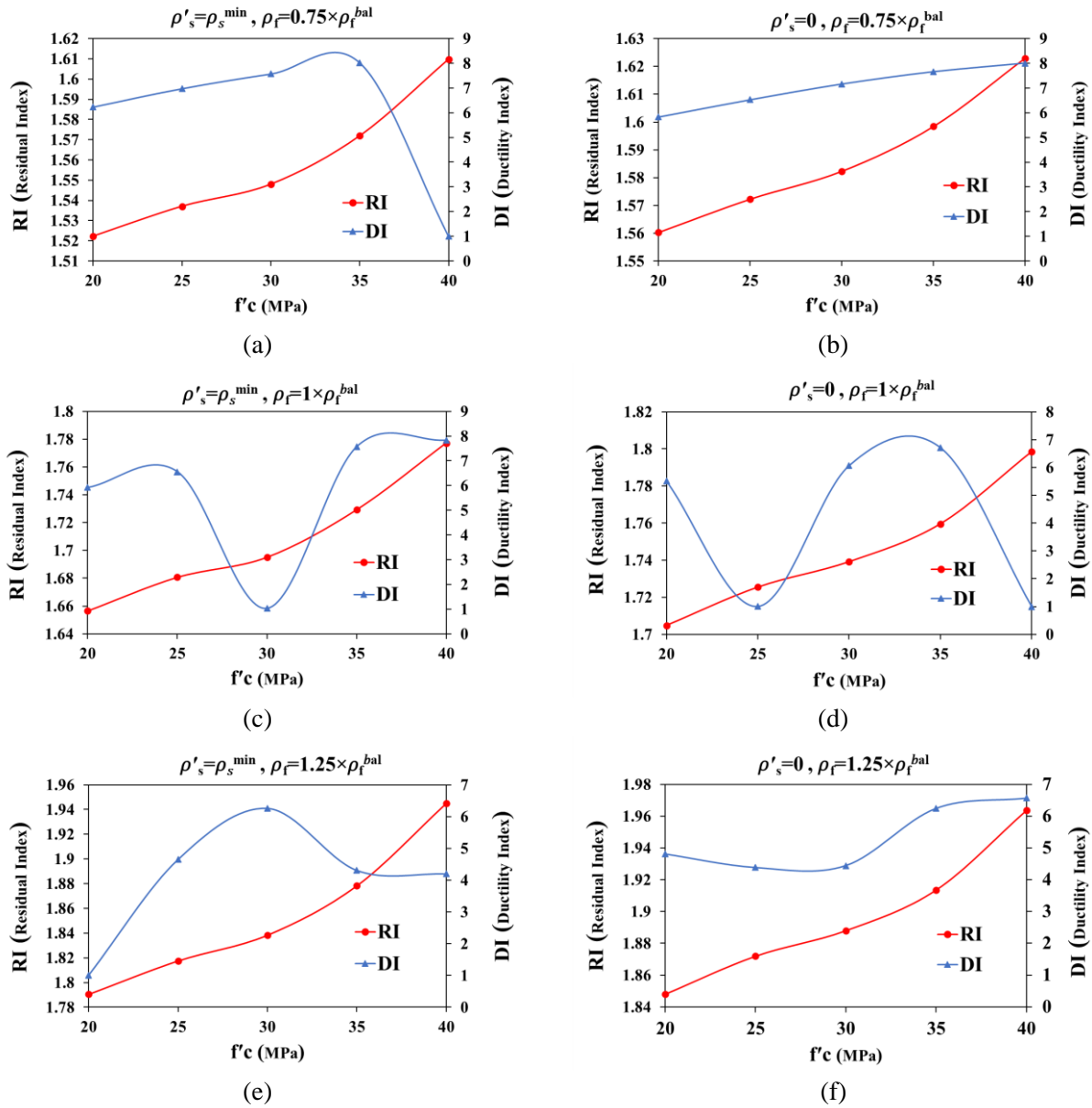


Fig. 9. Effect of compressive strength of concrete on ductility and residual indices ( $f_y = 400$  MPa,  $\rho_s = \rho_s^{min}$ ).

#### 5.4. Effect of the yield stress of steel bars on ductility and residual indices

The effect of the yield stress of steel bars ( $f_y$ ) on the ductility and residual indices has been investigated in different parts of Fig. 10. In these figures, the percentage of FRP bars and the percentage of steel compression bars are variable, but the fixed value  $\rho_s = \rho_s^{min}$  is assumed for the percentage of the steel tensile bars. It is also assumed that  $f'_c = 35$  MPa, and the composite bars are made of GFRP material. Based on the discussions made in subsections 5.2 and 5.3, it was proven that the selection of  $f'_c = 35$  MPa and  $\rho_s = \rho_s^{min}$  is the most favorable choice for getting maximum ductility and minimum residual deformations in HSF-reinforced concrete beams.

As seen in Fig. 10, the residual index of HSF-reinforced concrete beams increases with increasing the yield stress of steel bars. So, to reduce residual deformations in the beams, choosing steel bars with a yield stress of  $f_y = 500$  Mpa is the best option. However, the variations of the ductility index  $\mu$  against the changes of yield stress are different from the variations of residual index  $R$ . It is seen that the ductility

index of all HSF-reinforced concrete beams, except those beams with  $\rho'_s = \rho_s^{min}$  and  $\rho_f = 0.75 \times \rho_f^{bal}$ , decreases with increasing the yield stress of the steel bars. In the HSF-reinforced concrete beams with  $\rho'_s = \rho_s^{min}$  and  $\rho_f = 0.75 \times \rho_f^{bal}$ , the ductility index increases until around  $f_y = 400$  MPa, and then it decreases. Thus, by considering the reverse trend of the ductility index  $\mu$  and residual index R against  $f_y$ , one can deduce that the value of  $f_y = 400$  MPa is the best choice for the yield stress of steel bars. It is worth to mention that high-yield rebars can be more challenging to weld due to their increased carbon content and other alloying elements. This can limit their use in applications where welding is required for connections or splices. High-yield stress rebars are typically more expensive due to the specialized manufacturing processes and materials required to achieve higher strength. They may also be less readily available, depending on the region.

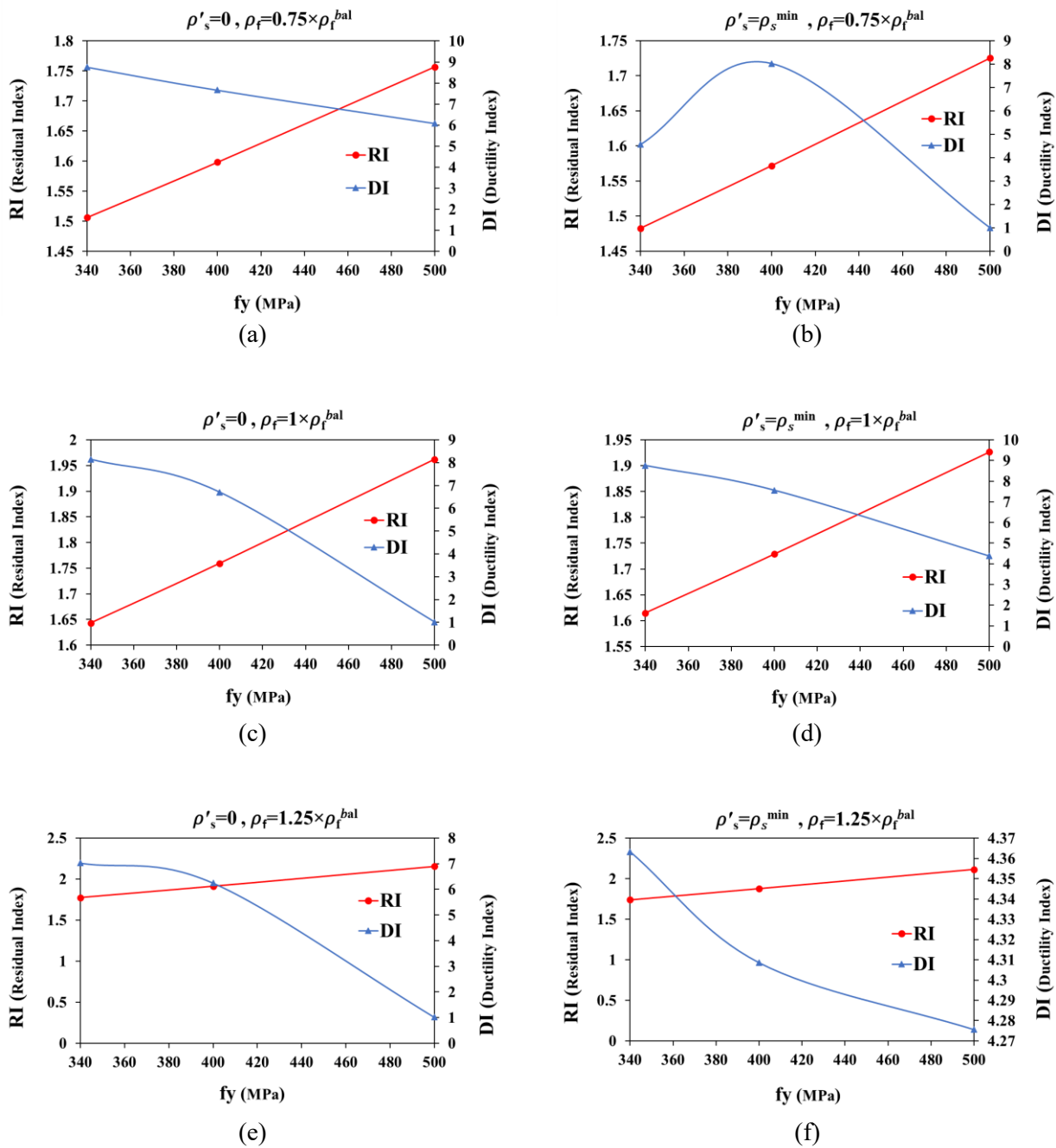


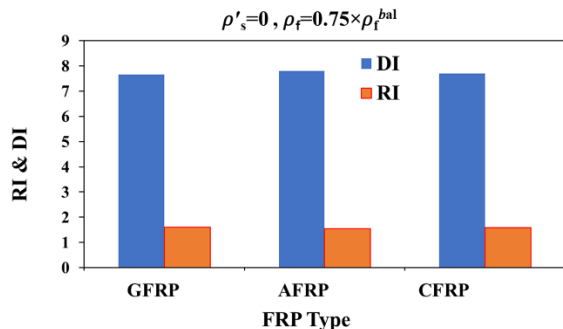
Fig. 10. Effect of the yield stress of steel bars on ductility and residual indices ( $f'_c = 35 \text{ MPa}$ ,  $\rho_s = \rho_s^{min}$ ).

### 5.5. Effect of the type of FRP composite bars on ductility and residual indices

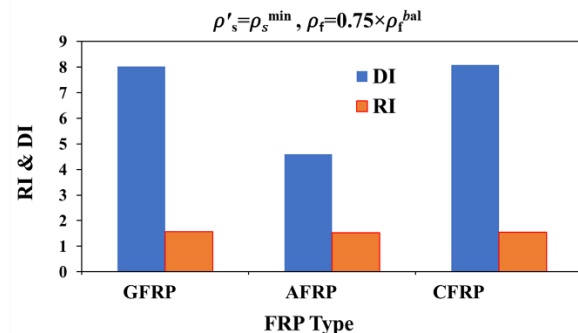
In this subsection, the effect of the type of FRP composite bars on the ductility and residual indices of HSF-reinforced concrete beams has been investigated. Three different types, including GFRP ( $E_{frp} = 41.4 \text{ GPa}$ ,  $f_u = 552 \text{ MPa}$ ,  $\varepsilon_{frp,u} = 1.33\%$ ), CFRP ( $E_{frp} = 152 \text{ GPa}$ ,  $f_u = 2070 \text{ MPa}$ ,  $\varepsilon_{frp,u} = 1.36\%$ ), and AFRP ( $E_{frp} = 82.7 \text{ GPa}$ ,  $f_u = 1172 \text{ MPa}$ ,  $\varepsilon_{frp,u} = 1.42\%$ ), are assumed for composite bars. The obtained results are shown in Table 3 and bar charts of Fig. 11. In these figures, the percentage of FRP composite bars and the percentage of steel compression bars are variable, but it assumed that  $f'_c = 35 \text{ MPa}$ ,  $f_y = 400 \text{ MPa}$ ,  $\rho_s = \rho_s^{min}$ .

**Table 3.** Effect of FRP type on  $\mu$  and  $R$ .

FRP type	$\rho_s$	$\rho_f$	$\mu$	R
GFRP	0	$0.75 \times \rho_f^{bal}$	7.663	1.598
AFRP	0	$0.75 \times \rho_f^{bal}$	7.806	1.545
CFRP	0	$0.75 \times \rho_f^{bal}$	7.694	1.580
GFRP	0	$1 \times \rho_f^{bal}$	6.707	1.760
AFRP	0	$1 \times \rho_f^{bal}$	3.540	1.695
CFRP	0	$1 \times \rho_f^{bal}$	6.270	1.739
GFRP	0	$1.25 \times \rho_f^{bal}$	6.249	1.914
AFRP	0	$1.25 \times \rho_f^{bal}$	6.378	1.839
CFRP	0	$1.25 \times \rho_f^{bal}$	6.297	1.887
GFRP	$\rho_s^{min}$	$0.75 \times \rho_f^{bal}$	8.025	1.572
AFRP	$\rho_s^{min}$	$0.75 \times \rho_f^{bal}$	4.588	1.523
CFRP	$\rho_s^{min}$	$0.75 \times \rho_f^{bal}$	8.078	1.556
GFRP	$\rho_s^{min}$	$1 \times \rho_f^{bal}$	7.561	1.729
AFRP	$\rho_s^{min}$	$1 \times \rho_f^{bal}$	7.767	1.664
CFRP	$\rho_s^{min}$	$1 \times \rho_f^{bal}$	7.673	1.708
GFRP	$\rho_s^{min}$	$1.25 \times \rho_f^{bal}$	4.309	1.878
AFRP	$\rho_s^{min}$	$1.25 \times \rho_f^{bal}$	4.374	1.804
CFRP	$\rho_s^{min}$	$1.25 \times \rho_f^{bal}$	4.327	1.850



(a)



(b)

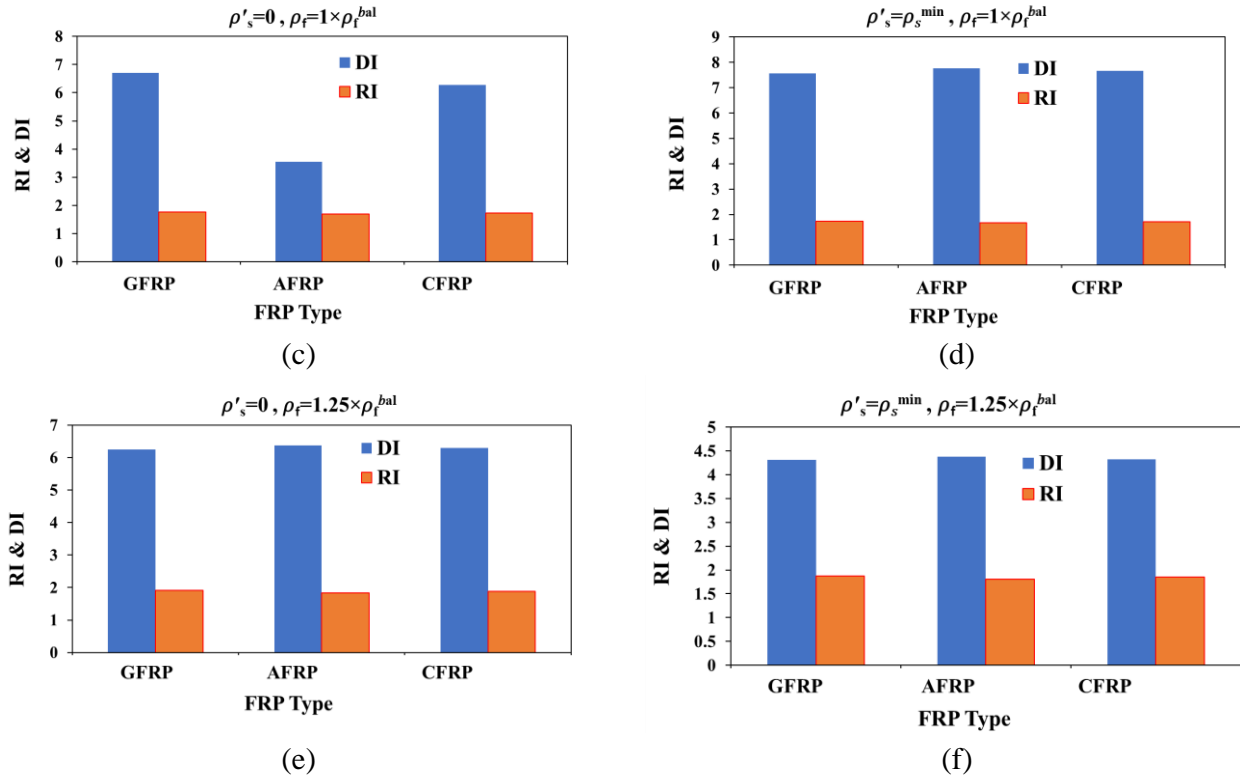


**Fig. 11.** Effect of various types of FRP bars on the ductility and residual indices ( $f'_c = 35 \text{ MPa}$ ,  $f_y = 400 \text{ MPa}$ ,  $\rho_s = \rho_s^{min}$ ).

As can be seen, the residual index of HSF-reinforced concrete beams is not so sensitive against the type of FRP composite bars. The use of GFRP composite bars leads to the highest value for the residual index, and the use of AFRP composite bars leads to the lowest value of this index. Therefore, if only the residual index is alone used as a selection criterion, the use of GFRP composite bars is the first choice, and choosing CFRP composite bars will be the next appropriate choice, which causes the least amount of residual deformations in the HSF-reinforced concrete beams.

If the ductility index is considered, it can be observed from the bar charts depicted in Fig. 11 that this index is not so sensitive against the type of FRP composite bars, except for the beams with  $\rho'_s=\rho_s^{min}$  and  $\rho_f=0.75 \times \rho_f^{bal}$ , and the beams with  $\rho'_s=0$  and  $\rho_f=1 \times \rho_f^{bal}$ . In the beams with  $\rho'_s=\rho_s^{min}$  and  $\rho_f=0.75 \times \rho_f^{bal}$ , and the beams with  $\rho'_s=0$  and  $\rho_f=1 \times \rho_f^{bal}$ , first, the use of GFRP composite bars and then, the use of CFRP composite bars leads to the highest value for the ductility parameter. According to the formulation outlined in Section 2, the moment-curvature relationship and, consequently, the ductility index of HSF-reinforced beams are complex functions of several parameters. These include the material properties of steel and FRP bars (such as modulus of elasticity and ultimate failure strain), the material properties of concrete, and the percentage ratios of FRP, steel, and compressive reinforcement. It seems that in the HSF-reinforced beams with  $\rho'_s=\rho_s^{min}$  and  $\rho_f=0.75 \times \rho_f^{bal}$ , as well as in the HSF-reinforced beams with  $\rho'_s=0$  and  $\rho_f=1 \times \rho_f^{bal}$ , the material properties of FRP bars, particularly the ultimate failure strain, plays a more dominant role in determining the ductility response. It is important to note that the ultimate failure strain of GFRP bars is lower than the ultimate failure strain of both CFRP and AFRP bars. Therefore, if only the ductility index is alone used as a selection criterion, the use of GFRP composite bars is the first choice, and choosing CFRP composite bars will be the next appropriate choice, which causes the highest energy absorption capacity in the HSF-reinforced concrete beams.

Concerning the economic aspects, GFRP bars are generally the least expensive among the FRP bars. CFRP bars are the most expensive among the FRP bars. AFRP bars fall between GFRP and CFRP bars in terms of cost.

Based on the argument mentioned in three previous paragraphs, it can be concluded that using GFRP composite bars is a suitable choice for concrete beams reinforced with a combination of steel and composite bars.

### 5.6. Effect of the percentage of steel compression bars on ductility and residual indices

The effect of the percentage of steel compression bars on the ductility and residual indices of HSF-reinforced concrete beams has been investigated in this subsection, and the obtained results are shown in Fig. 12. Three different reinforcement ratios  $\rho_f = 0.75 \times \rho_f^{bal}$ ,  $\rho_f = 1 \times \rho_f^{bal}$ , and  $\rho_f = 1.25 \times \rho_f^{bal}$  are considered for FRP composite bars. The value of the compressive strength of concrete is  $f'_c = 35 \text{ MPa}$ , the yield stress of steel bars is  $f_y = 400 \text{ MPa}$ , and the percentage of tensile steel bars is  $\rho_s = \rho_s^{min}$ . The type of composite bars is assumed to be the GFRP.

As shown in Fig. 12, the residual index of HSF-reinforced concrete beams decreases with increasing the percentage of compression bars. So, the best choice for the percentage of steel compression bars in HSF-reinforced concrete beams is  $\rho'_s = 0$  if the criterion of the minimum residual deformations is considered alone.

Concerning the ductility index, it can be seen from Fig. 12.a that the ductility index of beams with  $\rho_f = 0.75 \times \rho_f^{bal}$  is not sensitive to the changes in the percentage of steel compression bars. By increasing  $\rho'_s$  from 0 to  $1 \times \rho_s^{bal}$ , the value of the ductility index increases slightly from 7.66 to 11.13. In the concrete beams with  $\rho_f = 1 \times \rho_f^{bal}$  (see Fig. 12.b), the ductility index is almost insensitive to the percentage of the compression bars so that the value of the ductility index of these beams remains in the range of [6.2, 8]. Unlike the previous two cases, it can be seen that the ductility index of concrete beams with  $\rho_f = 1.25 \times \rho_f^{bal}$  is very sensitive to the changes in compression bars (see Fig. 12.c). With increasing the percentage of compression bars from 0 to 1, the value of the ductility index of these concrete beams reduced sharply from 6.2 to 1. It is clear that in this case, the absence of compression bars in the cross-section is the best choice for increasing the energy absorption capacity of the HSF-reinforced concrete beams. Altogether, it can be seen that the ductility index of some HSF-reinforced concrete beams is not sensitive to the changes in the percentage of steel compression bars. In concrete beams whose ductility index is sensitive to the amount of steel compression bars, the value of  $\rho'_s = 0$  leads to the maximum ductility index. Therefore, it can be deduced that the absence of steel compression bars in the cross-section is the best choice for getting the highest energy absorption capacity in the HSF-reinforced concrete beams.

If the criteria of maximum ductility and minimum residual deformations are simultaneously considered, according to the results obtained in two previous paragraphs, one can conclude that the value of  $\rho'_s = 0$  is the best choice for the amount of steel compression bars in HSF-reinforced concrete beams. However, due to the positive effect of steel compression bars in reducing creep deformations, and also due to the requirement of most the building codes for considering a minimum amount of compression bars in concrete beams, the value of  $\rho'_s = \rho_s^{min}$  is recommended for the design of concrete beams reinforced with hybrid steel/FRP bars. Indeed, removing compression bars from reinforced concrete structures poses significant structural risks. Without compression bars, HSF-reinforced beams may experience increased deflection under load due to the creep phenomenon. This can lead to excessive cracking and reduced

serviceability, affecting the functionality and safety of the structure. Additionally, it becomes more challenging for workers to install stirrups effectively in the absence of compression bars.

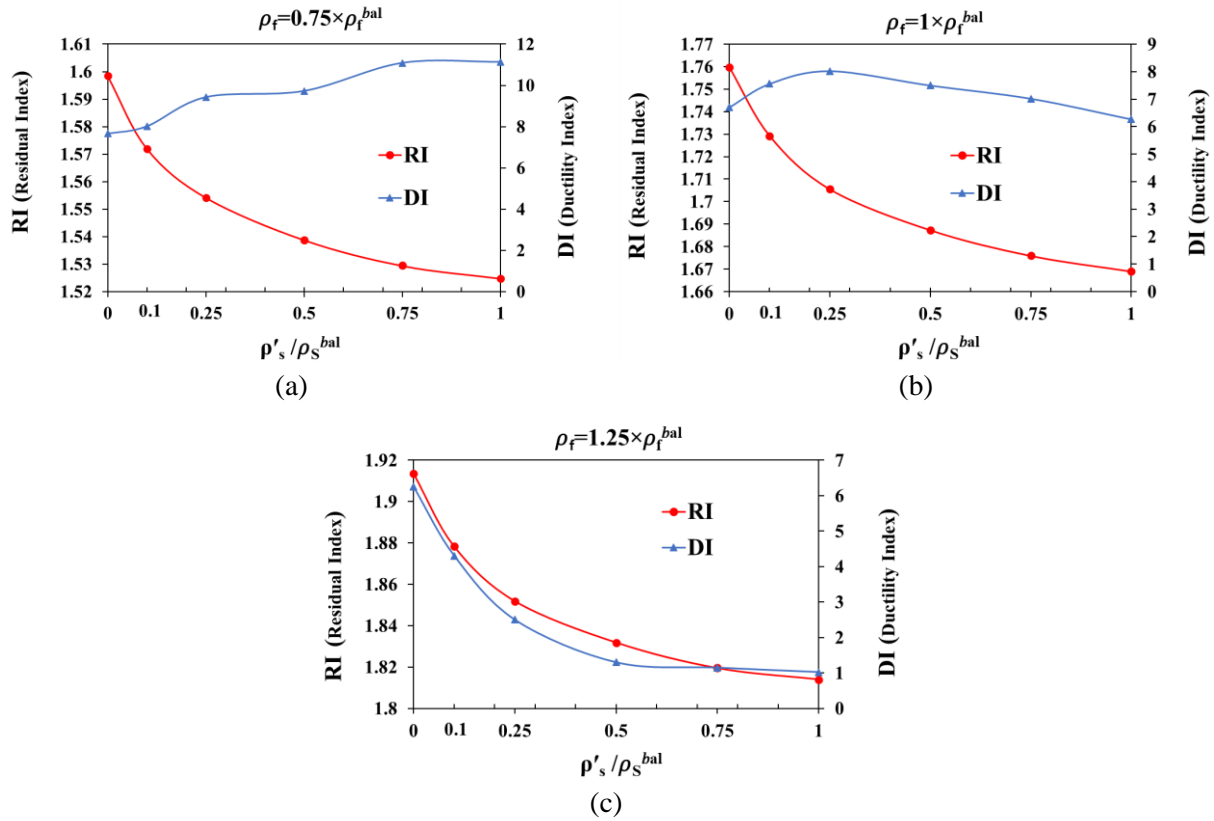


**Fig. 12.** Effect of the percentage of steel compression bars on ductility and residual indices ( $f'_c = 35 \text{ MPa}$ ,  $f_y = 400 \text{ MPa}$ ,  $\rho_s = \rho_s^{min}$ ).

### 5.7. HSF-reinforced concrete beams with optimal parameters

Based on the results obtained in subsections 5.1 to 5.6, the optimal values for the main parameters of HSF-reinforced concrete beams that lead to the best structural performance are briefly listed in Table 4.

**Table 4.** Optimal values for main parameters of HSF-reinforced concrete beams.

$f'_c$ (MPa)	$f_y$ (MPa)	Type of composite bars	$\rho'_s$	$\rho_s$	$\rho_f$
35	400	GFRP	0	$\rho_s^{min}$	$0.75 \times \rho_f^{bal}$
			$\rho_s^{min}$		$\rho_f^{bal}$
					$1.25 \times \rho_f^{bal}$

Table 5 shows the mechanical properties, reinforcing details, and structural responses of six HSF-reinforced concrete beams whose main parameters are optimum. In Table 5, the values of curvature, the ductility index, residual index, cracking moment, resistant bending moment, equal steel reinforcement ratio, and equal FRP reinforcement ratio for these beams are also shown and compared with each other. The equal steel reinforcement ratio and equal FRP reinforcement ratio are defined as Liu *et al.* [23]:

$$\rho_{steel}^{equ} = \rho_s + \left( \frac{f_{u,frp}}{f_y} \right) \rho_f \quad (17)$$

$$\rho_{FRP}^{equ} = \rho_f + \left( \frac{f_y}{f_{u,frp}} \right) \rho_s \quad (18)$$

It is observed from Table 5 that the HSF-reinforced concrete beams with optimal parameters have relatively similar structural performance. The discrepancies between the structural responses of the beams with optimal parameters are less than 10%.

**Table 5.** Details of six HSF-reinforced concrete beams with optimal parameters.

	H-1	H-2	H-3	H-4	H-5	H-6
$f'_c$ (MPa)	35	35	35	35	35	35
$f_y$ (MPa)	400	400	400	400	400	400
Type of FRP	GFRP	GFRP	GFRP	GFRP	GFRP	GFRP
$\rho'_s$ (%)	0	0	0	0.35	0.35	0.35
$\rho_s$ (%)	0.35	0.35	0.35	0.35	0.35	0.35
$\rho_f$ (%)	0.59	0.79	0.99	0.59	0.79	0.99
$\rho_{steel}^{equ}$ (%)	1.16	1.44	1.72	1.16	1.44	1.72
$\rho_{FRP}^{equ}$ (%)	0.84	1.04	1.24	0.84	1.04	1.24
$\varphi_u$ ( $\frac{1}{mm} \times 10^{-5}$ )	4.13	3.69	3.38	4.48	4.01	3.67
$\varphi_y$ ( $\frac{1}{mm} \times 10^{-5}$ )	0.54	0.55	0.54	0.56	0.53	0.85
$\varphi_R$ ( $\frac{1}{mm} \times 10^{-5}$ )	2.58	2.10	1.77	2.85	2.32	1.96
$\mu$	7.66	6.71	6.25	8.02	7.56	4.31
$R$	1.60	1.76	1.91	1.57	1.73	1.88
$M_{cr}$ (N.mm $\times 10^8$ )	1.59	1.66	1.73	1.60	1.70	1.76
$M_u$ (N.mm $\times 10^8$ )	4.53	5.07	5.53	4.81	5.41	5.92

\*\* Note:  $\rho_s^{min}=0.0035$ ,  $\rho_s^{bal}=0.036$   $\rho_f^{bal}=0.0079$

In Fig. 13, the moment-curvature diagrams of the HSF-reinforced concrete beams with optimal parameters are shown and compared with each other. According to Fig. 13, it is seen that the presence of steel compression bars (i.e., H-4, H-5, and H-6 samples) increases both the flexural capacity and the ultimate curvature of the HSF-reinforced concrete beams. However, as discussed in subsection 5.6, the presence of steel compression leads to the increase of residual deformations of HSF-reinforced concrete beams. Also, Fig. 13 shows that the increase in the percentage of FRP bars causes a significant increase in the flexural capacity of the HSF-reinforced concrete beams. Besides increasing the flexural capacity, the ultimate curvature of the HSF-reinforced concrete beams decreases by increasing the percentage of FRP bars. It was previously proved in subsection 5.1 that the increase in the FRP reinforcement ratio reduces both the energy absorption capacity and residual deformations of HSF-reinforced concrete beams.

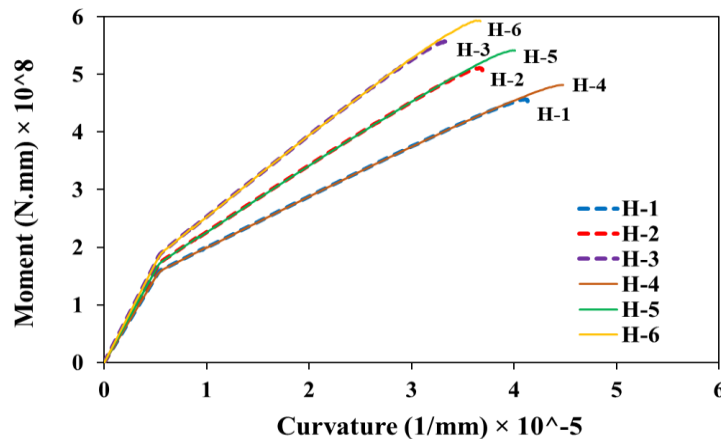


**Fig. 13.** Moment-curvature relationships in HSF-reinforced concrete beams with optimal parameters.

In the following, the structural behavior of six optimal HSF-reinforced concrete beams (i.e., H-1, H-2, H-3, H-4, H-5, and H-6) have been compared with the structural behavior of the concrete beams reinforced only with pure steel or pure FRP composite bars. The reinforcement details of these pure steel-reinforced concrete beams and pure FRP-reinforced concrete beams are given in Table 6. It should be noted that the reinforcement ratio in a concrete beam reinforced only with steel bars is equal to the sum of steel and FRP reinforcement ratios in the HSF-reinforced counterpart. Similarly, the reinforcement ratio in a concrete beam reinforced only with FRP bars is equal to the sum of the reinforcement ratio of steel and FRP in the HSF-reinforced counterpart. Other mechanical and geometrical characteristics of the steel- and FRP-reinforced concrete beams are the same as the mechanical and geometrical characteristics of their HSF-reinforced counterpart.

**Table 6.** Reinforcement details of steel- and FRP-reinforced concrete beams.

FRP-reinforced concrete beams				Steel-reinforced concrete beams				HSF-reinforced concrete beams			
Sample	$\rho'_s$ (%)	$\rho_s$ (%)	$\rho_f$ (%)	Sample	$\rho'_s$ (%)	$\rho_s$ (%)	$\rho_f$ (%)	Sample	$\rho'_s$ (%)	$\rho_s$ (%)	$\rho_f$ (%)
F-1	0	0	0.94	S-1	0	0.94	0	H-1	0	0.35	0.59
F-2	0	0	1.14	S-2	0	1.14	0	H-2	0	0.35	0.79
F-3	0	0	1.34	S-3	0	1.34	0	H-3	0	0.35	0.99
F-4	0.35	0	0.94	S-4	0.35	0.94	0	H-4	0.35	0.35	0.59
F-5	0.35	0	1.14	S-5	0.35	1.14	0	H-5	0.35	0.35	0.79
F-6	0.35	0	1.34	S-6	0.35	1.34	0	H-6	0.35	0.35	0.99

In Table 7, the values of the flexural capacity, the ductility index, and the residual index of pure steel RC beams and pure FRP RC beams are shown and compared with the corresponding values of their HSF-reinforced counterparts. As can be seen, the average flexural capacity of HSF-reinforced concrete beams is 31.8% larger than the average flexural capacity of pure steel RC beams, while it is 4.49% less than the average flexural capacity of pure FRP RC beams. The average residual index of HSF-reinforced concrete beams is 33.02% larger than the average residual index of pure steel RC beams, and it is 50.17% less than the average residual index of pure FRP RC beams. The average ductility index of HSF-reinforced concrete beams is 37.58% lower than pure steel RC beams, and it is 47.62% more than the average ductility index of pure FRP RC beams.

**Table 7.** Comparison of the structural responses of pure steel-reinforced concrete beams and pure FRP-reinforced concrete beams with their HSF-reinforced counterparts.

FRP-reinforced concrete beams				Steel-reinforced concrete beams				HSF-reinforced concrete beams			
Sample	R	$\mu$	$M_u$	Sample	R	$\mu$	$M_u$	Sample	R	$\mu$	$M_u$
F-1	2.88 (80.16%)	3.01 (-60.70%)	4.83 (6.62%)	S-1	1.11 (-30.63%)	9.82 (28.20%)	3.30 (-37.27%)	H-1	1.60	7.66	4.53
F-2	2.62 (48.86%)	3.32 (-50.52%)	5.27 (3.94%)	S-2	1.14 (-35.23%)	8.75 (30.40%)	4.01 (-26.43%)	H-2	1.76	6.71	5.07
F-3	2.45 (28.27%)	3.33 (-46.72%)	5.66 (2.35%)	S-3	1.18 (-38.22%)	8.01 (28.16%)	4.69 (-17.91%)	H-3	1.91	6.25	5.53
F-4	2.71 (72.29%)	3.52 (-56.11%)	5.16 (7.28%)	S-4	1.10 (-29.94%)	10.8 (34.66%)	3.29 (-46.20%)	H-4	1.57	8.02	4.81
F-5	2.52 (45.52%)	3.51 (-53.57%)	5.65 (4.44%)	S-5	1.12 (-35.26%)	9.69 (28.17%)	3.99 (-35.59%)	H-5	1.73	7.56	5.41
F-6	2.37 (25.93%)	3.53 (-18.10%)	6.06 (2.36%)	S-6	1.15 (-38.83%)	7.58 (75.87%)	4.66 (-27.04%)	H-6	1.88	4.31	5.92



For a better comparison, the moment-curvature relationships of H-1, S-1, and F-1 beams are shown in Fig. 14. It can be seen that the structural behavior of the H-1 beam is to some extent the intermediate of structural responses of S-1 and F-1 beams. Similar results will be observed if the moment-curvature diagrams are depicted for other beams. Therefore, by using the optimal design parameters found in this study, it is possible to increase the flexural capacity, the desired ductility, and the corrosion resistance of the concrete beams. Moreover, the residual deformations may be significantly reduced if the HSF-reinforced concrete beams are designed based on the six optimal parameters found in the present study. For practical design purposes, it is advisable to determine the design parameters of the HSF-reinforced beam in accordance with the findings of this study to ensure optimal ductility and minimal residual deformations. Following this, the width and depth of the HSF-reinforced beam can be modified to achieve the required bending capacity.

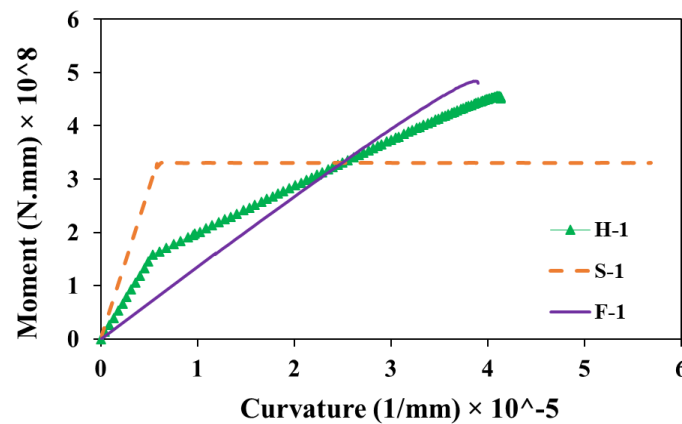


Fig. 14. Comparison of the moment-curvature relationships: H-1, S-1, and F-1 beam.

Concerning the economic considerations of HSF-reinforced concrete beams, they offer a cost-effective solution by combining the advantages of both materials. While the initial costs may be higher than pure steel beams, the long-term savings in maintenance and enhanced durability can make hybrid beams more economical over the life of the structure. Compared to pure FRP-reinforced beams, hybrid beams provide a more balanced performance at a lower initial cost. The choice between hybrid-, pure steel-, or pure FRP-reinforced beams should be based on a comprehensive evaluation of project requirements, including load conditions, environmental exposure, and long-term performance expectations.

## 6. Conclusions

The structural performance of HSF-reinforced concrete beams is affected by different parameters such as the percentage of steel/FRP bars, the percentage of steel compression bars, the type of FRP composite bars, the yield stress of steel bars, and concrete strength. In the present study, an attempt was made to determine the best combination of steel/FRP bars. To reach this aim, the sectional analysis of a series of HSF-reinforced concrete beams whose main parameters are different from each other was carried out, and their moment-curvature relationships were determined. To find the optimal percentage of steel/FRP bars and other main parameters, the moment-curvature curves of the analyzed HSF-reinforced concrete beams were compared with each other. Maximizing the energy absorption capacity and minimizing the effects of residual deformations after reloading are two criteria employed for determining the optimal parameters of HSF-reinforced concrete beams. The main results obtained from the present study are summarized as follows:

- The simultaneous use of steel and FRP composite bars significantly reduces the residual deformations of RC beams.

- The optimal percentages of FRP composite bars in HSF-reinforced concrete beams for getting the highest ductility and the lowest rate of residual deformations are  $\rho_f=0.75\times\rho_f^{bal}$  and  $\rho_f=1\times\rho_f^{bal}$  and  $\rho_f=1.25\times\rho_f^{bal}$ . The optimal percentage of steel tensile bars is equal to  $\rho_s = \rho_s^{min}$ . This value for steel compression bars is  $\rho'_s=0$  and  $\rho'_s = \rho_s^{min}$ .
- Using concrete with compressive strength of  $f'_c=35$  MPa, steel bars with the yield stress of  $f_y=400$  MPa, and composite bars made of GFRP leads to the most suitable structural performance in HSF-reinforced concrete beams.
- The residual deformations in HSF-reinforced concrete beams increase by increasing the percentage of steel compression bars.
- By increasing the percentage of FRP composite bars, the amount of residual deformations of HSF-reinforced concrete beam decreases.
- Compared to pure steel-reinforced concrete beams, the average flexural capacity of the HSF-reinforced concrete beams with optimal parameters is 31.8% larger. However, the average flexural capacity of the HSF-reinforced concrete beams with optimal parameters is 4.49% lower than the flexural capacity of pure FRP-reinforced concrete beams.
- The average residual index of the HSF-reinforced concrete beams with optimal parameters is 33.02% larger than the average residual index of pure steel-reinforced concrete beams. Compared to pure FRP-reinforced concrete beams, the average residual index of the HSF-reinforced concrete beams with optimal parameters is 50.17% less.
- The average ductility index of HSF-reinforced concrete beams with optimal parameters is 37.58% lower than the average ductility index of pure steel-reinforced concrete beams, and it is 47.62% larger than the average ductility index of pure FRP-reinforced concrete beams.

The present study has some limitations. For sectional analysis of HSF-reinforced concrete beams, it is assumed that the planes perpendicular to the longitudinal axis of the beam remain plane, implying a linear variation of strain across the cross-section of the beam. However, in deep concrete beams with a length-to-depth ratio of less than 2, the strain does not vary linearly along the cross-section, even under small loading conditions. Consequently, the findings of this study are not applicable to the optimal design of deep HSF-reinforced concrete beams. Addressing these limitations is recommended for future research. Experimental investigation of the structural behaviors of HSF-reinforced concrete beams that are fabricated based on the obtained optimal parameters of the present study is another subject that is recommended for future research.

## Funding

This research did not receive any specific grant from funding agencies in the public, commercial, or not-for-profit sectors.

## Conflicts of interest

The authors declare that they have no known competing financial interests or personal relationships that could have appeared to influence the work reported in this paper.

## Authors contribution statement

**K. Karami:** Formal analysis; Project administration; Software; Validation; Writing-original draft.

**J. Shafaei:** Investigation; Methodology; Supervision; Validation; Writing-review & editing.

**M. Lezgy-Nazargah:** Validation; Writing-original draft; Writing-review & editing.

## References

- [1] Moazzenchi S, Oskouei AV. A Comparative Experimental Study on the Flexural Behavior of Geopolymer Concrete Beams Reinforced with FRP Bars. *J Rehabil Civ Eng* 2023;11:21–42. <https://doi.org/10.22075/JRCE.2022.25157.1569>.
- [2] Shirmardi MM, Mohammadzadeh MR. Numerical Study on the Flexural Behaviour of Concrete Beams Reinforced by GFRP Bars. *J Rehabil Civ Eng* 2019;7:88–99. <https://doi.org/10.22075/JRCE.2018.14701.1268>.
- [3] Gopal R, Krishnachandran S. Flexural behaviour of RC beams substituted with GFRP reinforcement in aggressive environments. *Mag Concr Res* 2021;73:865–78. <https://doi.org/10.1680/jmacr.19.00285>.
- [4] Moolaei S, Sharbatdar MK, Kheyroddin A. Experimental evaluation of flexural behavior of HPFRCC beams reinforced with hybrid steel and GFRP bars. *Compos Struct* 2021;275:114503. <https://doi.org/10.1016/j.compstruct.2021.114503>.
- [5] Pilakoutas K, Guadagnini M, Neocleous K, Matthys S. Design guidelines for FRP reinforced concrete structures. *Proc Inst Civ Eng Struct Build* 2011;164:255–63. <https://doi.org/10.1680/stbu.2011.164.4.255>.
- [6] Yang Y, Pan D, Wu G, Cao D. A new design method of the equivalent stress–strain relationship for hybrid (FRP bar and steel bar) reinforced concrete beams. *Compos Struct* 2021;270:114099. <https://doi.org/10.1016/j.compstruct.2021.114099>.
- [7] Hussein A, Huang H, Okuno Y, Wu Z. Experimental and numerical parametric study on flexural behavior of concrete beams reinforced with hybrid combinations of steel and BFRP bars. *Compos Struct* 2022;302:116230. <https://doi.org/10.1016/j.compstruct.2022.116230>.
- [8] Johnson J, Xu M, Jacques E. Predicting the self-centering behavior of hybrid FRP-steel reinforced concrete beams under blast loading. *Eng Struct* 2021;247:113117. <https://doi.org/10.1016/j.engstruct.2021.113117>.
- [9] Taerwe L. FRP bars and the elimination of reinforcement corrosion in concrete structures. *Non-Metallic Reinf. Concr. Struct.*, CRC Press; 2004, p. 245–52.
- [10] Tan K. Behavior of hybrid FRP-steel reinforced concrete beams. *Third Int. Symp. Non-Metallic Reinf. Concr. Struct.*, Sapporo Japan: 1997, p. 479–87.
- [11] Antonietta AM, Luciano O. Structural Performances of Concrete Beams with Hybrid (Fiber-Reinforced Polymer-Steel) Reinforcements. *J Compos Constr* 2002;6:133–40. [https://doi.org/10.1061/\(ASCE\)1090-0268\(2002\)6:2\(133\)](https://doi.org/10.1061/(ASCE)1090-0268(2002)6:2(133)).
- [12] Leung HY, Balendran R V. Flexural behaviour of concrete beams internally reinforced with GFRP rods and steel rebars. *Struct Surv* 2003;21:146–57. <https://doi.org/10.1108/02630800310507159>.
- [13] Qu W, Zhang X, Huang H. Flexural Behavior of Concrete Beams Reinforced with Hybrid (GFRP and Steel) Bars. *J Compos Constr* 2009;13:350–9. [https://doi.org/10.1061/\(asce\)cc.1943-5614.0000035](https://doi.org/10.1061/(asce)cc.1943-5614.0000035).
- [14] Sun ZY, Yang Y, Qin WH, Ren ST, Wu G. Experimental study on flexural behavior of concrete beams reinforced by steel-fiber reinforced polymer composite bars. *J Reinf Plast Compos* 2012;31:1737–45. <https://doi.org/10.1177/0731684412456446>.
- [15] El Refai A, Abed F, Al-Rahmani A. Structural performance and serviceability of concrete beams reinforced with hybrid (GFRP and steel) bars. *Constr Build Mater* 2015;96:518–29. <https://doi.org/10.1016/j.conbuildmat.2015.08.063>.
- [16] Pang L, Qu W, Zhu P, Xu J. Design Propositions for Hybrid FRP-Steel Reinforced Concrete Beams. *J Compos Constr* 2016;20:4015086. [https://doi.org/10.1061/\(asce\)cc.1943-5614.0000654](https://doi.org/10.1061/(asce)cc.1943-5614.0000654).
- [17] Qin R, Zhou A, Lau D. Effect of reinforcement ratio on the flexural performance of hybrid FRP reinforced concrete beams. *Compos Part B Eng* 2017;108:200–9. <https://doi.org/10.1016/j.compositesb.2016.09.054>.
- [18] Lau D, Pam HJ. Experimental study of hybrid FRP reinforced concrete beams. *Eng Struct* 2010;32:3857–65. <https://doi.org/10.1016/j.engstruct.2010.08.028>.
- [19] Mustafa SAA, Hassan HA. Behavior of concrete beams reinforced with hybrid steel and FRP composites. *HBRC J* 2018;14:300–8. <https://doi.org/10.1016/j.hbrj.2017.01.001>.

- [20] Sun Z, Fu L, Feng D-C, Vatuloka AR, Wei Y, Wu G. Experimental study on the flexural behavior of concrete beams reinforced with bundled hybrid steel/FRP bars. *Eng Struct* 2019;197:109443. <https://doi.org/https://doi.org/10.1016/j.engstruct.2019.109443>.
- [21] Kim S, Kim S. Flexural behavior of concrete beams with steel bar and FRP reinforcement. *J Asian Archit Build Eng* 2019;18:94–102. <https://doi.org/10.1080/13467581.2019.1596814>.
- [22] Ge W, Wang Y, Ashour A, Lu W, Cao D. Flexural performance of concrete beams reinforced with steel–FRP composite bars. *Arch Civ Mech Eng* 2020;20:56. <https://doi.org/10.1007/s43452-020-00058-6>.
- [23] Liu S, Wang X, Ali YMS, Su C, Wu Z. Flexural behavior and design of under-reinforced concrete beams with BFRP and steel bars. *Eng Struct* 2022;263:114386. <https://doi.org/10.1016/j.engstruct.2022.114386>.
- [24] Hognestad E, Hanson N, McHenry D. Concrete stress distribution in ultimate strength design. *ACI J* 1955;52:455–480.
- [25] Zhou B, Wu R-Y, Liu Y, Zhang X, Yin S. Flexural Strength Design of Hybrid FRP-Steel Reinforced Concrete Beams. *Materials (Basel)* 2021;14. <https://doi.org/10.3390/ma14216400>.
- [26] ACI 440.11-22: Building Code Requirements for Structural Concrete Reinforced with Glass Fiber-Reinforced Polymer (GFRP) Bars—Code and Commentary. 2022.
- [27] ACI 318-19(22): Building Code Requirements for Structural Concrete. 2022.
- [28] Moehle J. *Seismic Design of Reinforced Concrete Buildings*. 1st Editio. New York: McGraw-Hill Education; 2015.
- [29] Kara IF, Ashour AF, Köroğlu MA. Flexural behavior of hybrid FRP/steel reinforced concrete beams. *Compos Struct* 2015;129:111–21. <https://doi.org/10.1016/j.compstruct.2015.03.073>.